© 2018. Published by The Company of Biologists Ltd | Journal of Cell Science (2018) 131, jcs204750. doi:10.1242/jcs.204750

RESEARCH ARTICLE

Dual role of the RNA helicase DDX5 in post-transcriptional regulation of myelin basic protein in oligodendrocytes

Peter Hoch-Kraft[1], Robin White[1,2], Stefan Tenzer[3], Eva-Maria Krämer-Albers[1], Jacqueline Trotter[1,*] and Constantin Gonsior[1,*]

ABSTRACT

In the central nervous system, oligodendroglial expression of myelin basic protein (MBP) is crucial for the assembly and structure of the myelin sheath. MBP synthesis is tightly regulated in space and time, particularly at the post-transcriptional level. We have identified the DEAD-box RNA helicase DDX5 (also known as p68) in a complex with *Mbp* mRNA in oligodendroglial cells. Expression of DDX5 is highest in progenitor cells and immature oligodendrocytes, where it localizes to heterogeneous populations of cytoplasmic ribonucleoprotein (RNP) complexes associated with *Mbp* mRNA in the cell body and processes. Manipulation of the amount of DDX5 protein inversely affects the level of MBP. We present evidence that DDX5 is involved in post-transcriptional regulation of MBP protein synthesis, with implications for oligodendroglial development. In addition, knockdown of DDX5 results in an increased abundance of MBP isoforms containing exon 2 in immature oligodendrocytes, most likely by regulating alternative splicing of *Mbp*. Our findings contribute to the understanding of the complex nature of MBP post-transcriptional control in immature oligodendrocytes where DDX5 appears to affect the abundance of MBP proteins via distinct but converging mechanisms.

KEY WORDS: Oligodendrocyte, DDX5, RNA helicase, Myelin basic protein, MBP exon 2, Post-transcriptional regulation

INTRODUCTION

Oligodendrocytes are the myelinating cells of the central nervous system (CNS) and ensure fast propagation of saltatory signals and integrity of the neuronal network (Nave, 2010; Nave and Werner, 2014). Mature oligodendrocytes differentiate from oligodendrocyte precursor cells (OPCs) to form multipolar cells that enwrap individual axonal segments, resulting in myelination in the CNS (Bercury and Macklin, 2015; Hughes and Appel, 2016; Mitew et al., 2014). Myelin loss or dysfunction contributes to development of neurological disorders such as multiple sclerosis (Compston and Coles, 2008; Ffrench-Constant, 1994; Franklin et al., 2012) and other leukodystrophies (Duncan and Radcliff, 2016). Increasing evidence also suggests a role of myelin abnormalities in various neurodegenerative diseases (Ettle et al., 2015; Kang et al., 2013) and psychiatric disorders (Fields, 2008; Poggi et al., 2016).

Myelin basic protein (MBP), one of the major structural myelin proteins, is indispensable for the formation of compact myelin in the CNS. Classical functions of MBP encompass myelin membrane assembly and organization (Aggarwal et al., 2011; Bakhti et al., 2014; Fitzner et al., 2006; Harauz and Boggs, 2013; Nawaz et al., 2015), including compaction of the myelin bilayer by phase transition of soluble MBP molecules into a liquid-like meshwork upon membrane association (Aggarwal et al., 2013). Consequently, *shiverer* mouse mutants lacking MBP show a severe dysmyelination phenotype (Readhead and Hood, 1990) and abnormal cellular properties of oligodendrocytes *in vitro* (Dyer et al., 1995; Seiwa et al., 2002). Murine *Mbp* transcripts arise from a locus called *genes of oligodendrocyte lineage* (*golli*) on chromosome 18 and alternative splicing of exon 2 and exon 5/6 generates the classical MBP isoforms ranging from 14 kDa to 21.5 kDa (Boggs, 2006; Campagnoni et al., 1993).

While classical exon 2-negative isoforms localize primarily to the oligodendroglial plasma membrane, exon 2-positive isoforms (17.2 kDa, 21.5 kDa) exhibit cytosolic and nuclear localization patterns (Allinquant et al., 1991; Hardy et al., 1996; Pedraza et al., 1997; Staugaitis et al., 1996). They have been shown to exert signaling functions including an enhancement of oligodendroglial proliferation and increased process outgrowth of co-cultured neuronal cells (Smith et al., 2013).

Synthesis of MBP protein is strictly regulated by post-transcriptional mechanisms, which control the correct temporal and spatial expression of the protein (Carson et al., 2008; Müller et al., 2013). *Mbp* mRNA is found in the myelin compartment (Colman et al., 1982; Thakurela et al., 2016) and is one of the first reported examples of transport and localized translation of mRNA in the nervous system (Ainger et al., 1993). Binding of hnRNP A2/B1 to the A2 response element (A2RE) in the *Mbp* 3′UTR (Ainger et al., 1997; Han et al., 2010; Hoek et al., 1998; Martinez et al., 2016; Munro et al., 1999) favors formation of cytoplasmic transport granules and mediates translocation to the cellular periphery on the microtubule network (Carson et al., 1997; Seiberlich et al., 2015). Several factors have been identified as structural and functional components of *Mbp* mRNA-associated complexes, including components of the protein translation machinery (Barbarese et al., 1995), motor proteins (Lyons et al., 2009; Herbert et al., 2017), the microtubule-associated TOG (Francone et al., 2007; Kosturko et al., 2005; Maggipinto et al., 2017), hnRNP E1 (PCBP1) and hnRNP K (Kosturko et al., 2006; Laursen et al., 2011; Torvund-Jensen et al., 2014), hnRNP F (White et al., 2012), the hnRNP A/B-related protein CBF-A (Raju et al., 2008) and Argonaute-2 (Müller et al., 2015). A hallmark of localized mRNAs is the robust inhibition of translation (Boccaccio, 2000; Eliscovich and Singer, 2017), which in *Mbp* mRNA-associated complexes is supported by hnRNP E1

[1]Molecular Cell Biology, Institute for Developmental Biology and Neurobiology, Department of Biology, Johannes Gutenberg-University of Mainz, Anselm-Franz-von-Bentzelweg 3, 55128 Mainz, Germany. [2]Institute of Physiology and Pathophysiology, University Medical Center of the Johannes Gutenberg-University, Duesbergweg 6, 55128 Mainz, Germany. [3]Institute for Immunology, University Medical Center Mainz, Langenbeckstr. 1, 55131 Mainz, Germany.

*Authors for correspondence (trotter@uni-mainz.de; gonsior@uni-mainz.de)

R.W., 0000-0003-4890-7202; J.T., 0000-0002-8336-8438; C.G., 0000-0003-0780-8654

Received 31 March 2017; Accepted 28 March 2018

Journal of Cell Science (2018) 131, jcs204750. doi:10.1242/jcs.204750

(PCBP1) (Kosturko et al., 2006) or small non-coding RNA 715 (Bauer et al., 2012). *Mbp* translational inhibition can be released by axonal signals, including neuronal activity, which mediate Fyn kinase-dependent *Mbp* translation at the axoglial interface (Laursen et al., 2009; Wake et al., 2011; White et al., 2008). Thereby, myelination of electrically active axons is preferentially promoted (Wake et al., 2015) potentially also contributing to activity-dependent myelin plasticity (Fields, 2015; Purger et al., 2016).

A proteomic screen for hnRNP A2/B1-associated proteins yielded the DEAD-box RNA helicase DDX5 as a potential novel interaction partner of *Mbp* mRNA. This multifunctional RNA-binding protein (RBP) is an ATP-dependent RNA helicase that has been shown to participate in various aspects of RNA biology from transcription to decay, including alternative splicing (Camats et al., 2008; Dardenne et al., 2014; Kar et al., 2011), miRNA processing (Hong et al., 2013; Suzuki et al., 2009) and transcriptional co-regulation (reviewed by Fuller-Pace, 2013). Here, we describe DDX5 as a component of *Mbp* mRNA-associated mRNP complexes in oligodendroglial cells, which contributes to post-transcriptional regulation of MBP protein expression. Furthermore, DDX5 knockdown affects the relative abundance of MBP exon 2-positive isoforms in pre-myelinating oligodendrocytes. Intriguingly, visualization of single *Mbp* mRNA molecules and associated proteins points to a heterogeneous composition of *Mbp* mRNPs, providing further insight into the complex post-transcriptional regulation of MBP expression in pre-myelinating oligodendrocytes.

RESULTS

DDX5 is associated with cytoplasmic *Mbp* mRNP complexes

Expression of MBP is a key step during oligodendrocyte maturation and hnRNP A2/B1 has been described as a central component of *Mbp* mRNA-containing cytoplasmic granules, binding directly to the A2RE in the 3′UTR of *Mbp* mRNA (Munro et al., 1999). In order to elucidate further constituents of *Mbp* mRNA granules, we immunopurified hnRNP A2/B1 from cytoplasmic extracts of Oli-*neu* cells and identified associated factors by SDS-PAGE and subsequent mass spectrometry of defined bands. One of the proteins we found was the DEAD-Box RNA helicase DDX5 (Fig. 1A). To confirm the binding of DDX5 to *Mbp* mRNA, we immunoprecipitated DDX5 from Oli-*neu* nuclei-depleted lysates and analyzed co-purifying mRNAs by qRT-PCR (Fig. 1B). We found that *Mbp* mRNA was enriched with cytoplasmic DDX5 compared with levels of control mRNAs, with a slight preference towards *Mbp* isoforms lacking exon 2. Interestingly, we could not routinely detect hnRNP A2/B1 co-purifying with DDX5 in these experimental conditions (Fig. 1B). To elucidate the spatiotemporal subcellular distribution of *Mbp* mRNA, we performed fluorescence *in situ* hybridization with single molecule sensitivity (smFISH) in developing primary mouse oligodendrocytes (Fig. 1C). In general, the number of *Mbp* transcripts increased dramatically during oligodendrocyte maturation from NG2-positive OPCs to mature oligodendrocytes and they were evenly distributed in the cell soma and processes (Fig. S1). Immunocytochemistry revealed DDX5 protein to be abundantly present in the nuclei and additionally revealed a granular pattern in the soma and the processes of the oligodendrocytes (Fig. 1F,H). In the cytoplasm, DDX5 protein showed a prominent granular colocalization with smFISH signals for *Mbp* mRNA in combined immunocytochemistry (Fig. 1D-J and Fig. 2H), further endorsing the association of DDX5 with cytoplasmic *Mbp* mRNA granules.

Heterogeneity of DDX5-containing cytoplasmic complexes

We further characterized cytoplasmic complexes containing DDX5 and *Mbp* mRNA by co-staining with hnRNP A2/B1 in primary oligodendrocytes (Fig. 2A-I). DDX5 signal partially colocalized with hnRNP A2/B1 in the oligodendroglial cytoplasm (Fig. 2G). Interestingly, DDX5 also showed an overlap with signals for *Mbp* mRNA in areas where hnRNP A2/B1 appeared to be absent (Fig. 2G-I), suggesting a novel DDX5-positive subpopulation of *Mbp* mRNA-containing cytoplasmic complexes. To analyze cytoplasmic RNPs biochemically, we subjected oligodendroglial cell extracts to Optiprep density gradient centrifugation (Fig. S2A) separating distinct RNP complexes according to their sedimentation velocity (Fritzsche et al., 2013). The spread of RBPs within the gradient indicates preservation of intact RNP complexes (Fig. 2J and Fig. S2B), as described before for Barentz and Staufen 2 in rat brain (Fritzsche et al., 2013). These complexes are disassembled upon RNase treatment, which results in a shift of RBP signals to the main protein peak in the lighter fractions (Fig. S2C). Analysis of mRNA levels by qRT-PCR revealed a relative enrichment of *Mbp* mRNA in heavier fractions 10-13 (Fig. 2K) which simultaneously contained markers for 60S and 40S ribosomal subunits (‘ribosome fractions’; Fig. 2J). In contrast, the mRNAs for phosphoglycerate kinase 1 (*Pgk1*) and 2′,3′-cyclic-nucleotide-3′-phosphodiesterase (*Cnp*) were highly enriched in the bottom fraction, suggesting an association of *Mbp* mRNA with complexes within the cytoplasm that differ from those containing *Pgk1* or *Cnp* mRNAs. DDX5 protein signal was present throughout the gradient and also in fractions containing ribosomal proteins (Fig. 2J and Fig. S2B), together with elevated levels of *Mbp* mRNA (Fig. 2K). In contrast, hnRNP A2/B1 was mainly detectable in light fractions and in the bottom fraction together with DDX5 (Fig. 2J and Fig. S2B). Taken together, the results of smFISH with combined immunofluorescence, RNA immunoprecipitation and different RBP sedimentation profiles suggest a heterogeneity of *Mbp* mRNA-associated complexes, at least with respect to the presence of DDX5 and hnRNP A2/B1.

DDX5 affects MBP protein expression at the post-transcriptional level

As it was found to be a novel component of *Mbp* mRNA-associated complexes, we analysed the function of DDX5 during early OL maturation in culture. Western blot analysis of primary oligodendrocytes showed that levels of DDX5 protein decreased during differentiation, whereas myelin protein levels (CNP, MBP) increased as expected (Fig. 3A). Strikingly, when we knocked down DDX5 using RNAi, we found a selective elevation of total MBP levels while levels of other oligodendroglial proteins were unaffected (Fig. 3B). Analysis of RBPs previously described in *Mbp* mRNA regulation (Müller et al., 2013) revealed that levels of hnRNP A2/B1 and F protein were moderately decreased upon DDX5 knockdown (Fig. 3C). Corresponding mRNA levels, including that of *Mbp*, remained unchanged (Fig. 3D), suggesting that DDX5 is involved both in the regulation of MBP and distinct *Mbp* mRNA-associated RBPs at the post-transcriptional level. We did not observe a change in the total number of MBP-positive cells upon depletion of DDX5 (Fig. S3A) and analysis of *Mbp* mRNA particle distribution after DDX5 knockdown did not show an alteration in the localization throughout the oligodendroglial cytoplasm (Fig. S3C), suggesting that DDX5 is not critical for translocation of *Mbp* mRNA granules to the periphery of the cell.

Oligodendroglial Fyn kinase activity has been shown to play a major role in neuron-dependent initiation of *Mbp* translation (Wake

Journal of Cell Science (2018) 131, jcs204750. doi:10.1242/jcs.204750

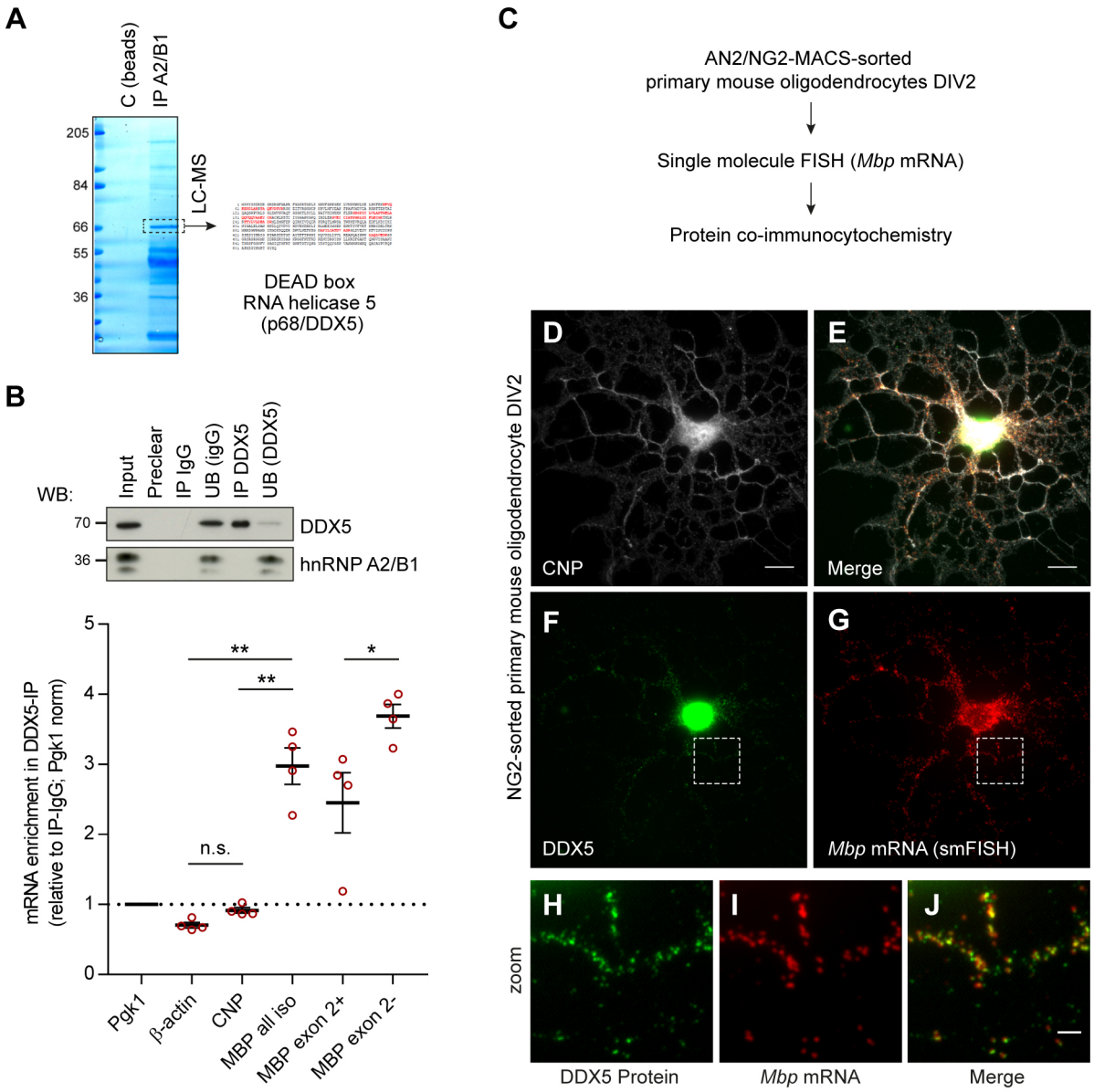

Fig. 1. DDX5 associates with *Mbp* mRNA in the cytoplasm of oligodendrocytes. (A) Proteins that co-precipitated with immunopurified hnRNP A2/B1 (IP A2B1) from cytoplasmic Oli-*neu* cell lysates were identified by LC-MS after excision of the indicated band from the gel and yielded the RNA helicase DDX5 as a potential component of *Mbp* mRNA-containing complexes. (B) *Mbp* mRNA enriches with DDX5 from the oligodendroglial cytoplasm. DDX5 immunoprecipitation from dbcAMP-differentiated Oli-*neu* PNS lysates was carried out using DDX5-specific (IP DDX5) or isotype-matched control (IP IgG) antibodies and analyzed by western blotting; UB, unbound proteins after immunoprecipitation. Co-purifying RNAs were extracted from the immunoprecipitations. Relative abundance of selected mRNAs was determined by qRT-PCR and mRNA enrichment in DDX5 immunoprecipitations was related to control IgG immunoprecipitations. Furthermore, genes of interest (*Mbp*, *Cnp*: myelin proteins, *β-actin*: localized mRNA) were related to the abundance of *Pgk1* mRNA (glycolytic enzyme). Individual data points are displayed as red circles. Black lines represent the mean from 4 individual experiments±s.e.m.; n.s. not significant, **P*<0.05, ***P*<0.01 (Student's *t*-test, paired, two-tailed). (C-J) MACS-sorted (anti-NG2) primary mouse oligodendrocytes at DIV 2 were subjected to Panomics smFISH using probes targeting *Mbp* mRNA and immunostained for DDX5 and CNP. Dashed boxes indicate regions in zoomed images H-J. DDX5 and *Mbp* mRNA colocalize in cytoplasmic granular foci in oligodendrocyte soma and processes. Scale bars: 10 µm (D-G) and 2 µm (H-J).

et al., 2011; White et al., 2008) and several factors regulating MBP expression at the post-transcriptional level have been shown to be phosphorylated by Fyn (Müller et al., 2013). We tested whether cytoplasmic DDX5 was subjected to Fyn-dependent phosphorylation using constitutive active and kinase-inactive Fyn constructs (White et al., 2012). However, no Fyn-dependent phosphorylation of DDX5 was observed, even after direct incubation of DDX5 with recombinant Fyn kinase (Fig. S3B), indicating that DDX5 is not a target in the Fyn-mediated *Mbp* translation regulatory pathway.

As DDX5 is an RNA helicase, a typical function is likely to include the manipulation of RNA secondary structures and RNA-protein interactions (Linder and Jankowsky, 2011). To investigate whether DDX5 affects MBP production via its ATP-dependent helicase activity, we generated the dominant negative ATP-binding-defective and helicase-inactive mutant DDX5^{K144N} (Jalal et al., 2007) by site-directed mutagenesis (Fig. 4A) and assessed myelin protein levels by western blotting in response to overexpression of mutant DDX5^{K144N} or wild-type DDX5^{WT} (Fig. 4B,C). Transfection

Journal of Cell Science (2018) 131, jcs204750. doi:10.1242/jcs.204750

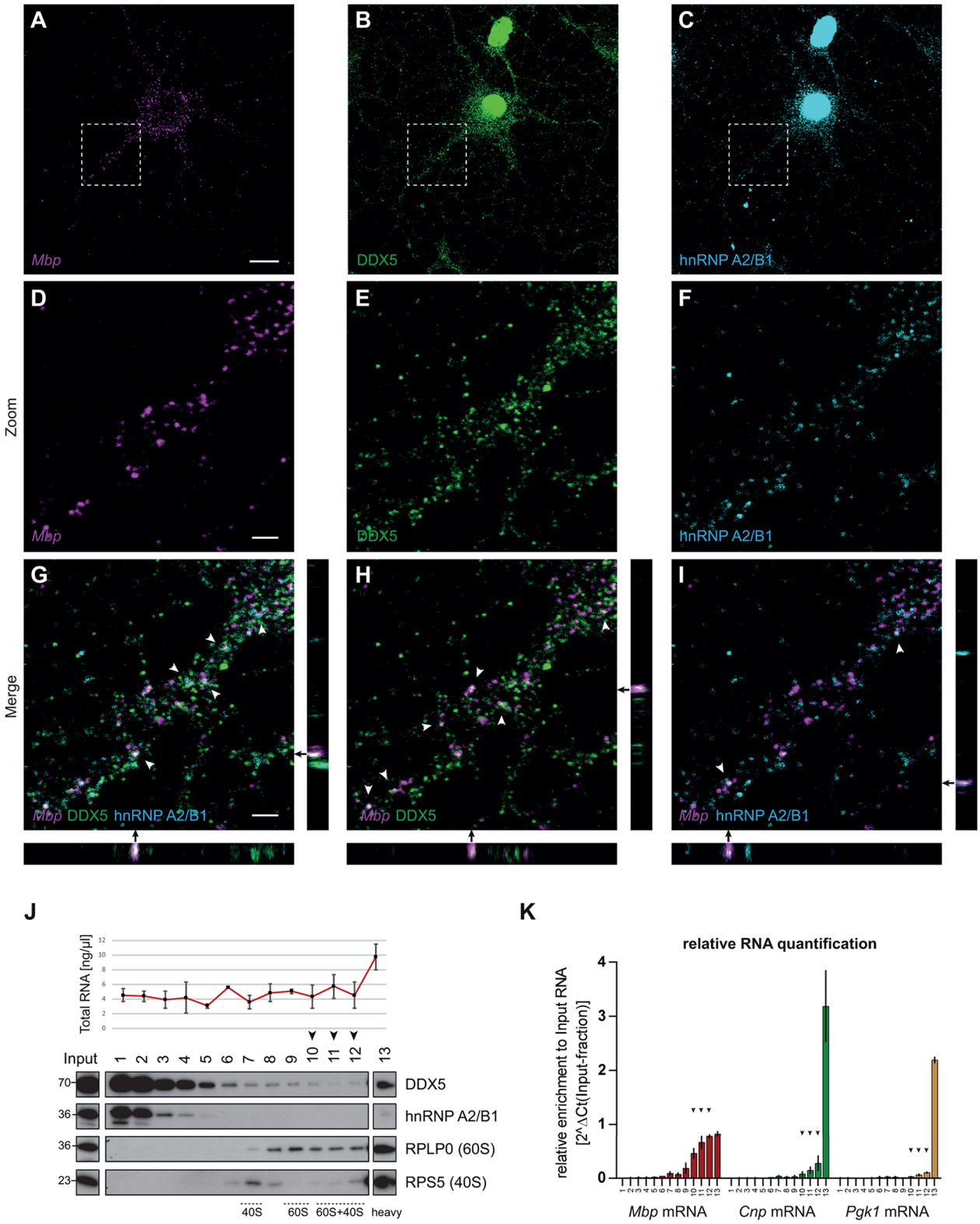

Fig. 2. Heterogeneity of cytoplasmic *Mbp* mRNPs in oligodendrocytes. (A-I) MACS-sorted (anti-NG2) primary mouse oligodendrocytes at DIV 2 were fixed, subjected to Panomics smFISH targeting *Mbp* mRNA and immunostained with specific antibodies for DDX5 and hnRNP A2/B1 (A-C). Confocal images were acquired using a Leica SP5 LSM. Individual focus planes are displayed. Scale bar: 10 µm. (D-I) Enlargements show granular foci in the cytoplasm where *Mbp* mRNA colocalizes with DDX5 (H) or hnRNP A2/B1 (I), with such foci being triple positive (G). *Z*-plane positions are indicated by black arrows. Scale bars: 5 µm. (J) Cytoplasmic extracts from MACS-sorted (anti-O4) primary mouse oligodendrocytes at DIV 5 were subjected to 5-25% Optiprep density gradient centrifugation and fractions (1-13) were analyzed by measurement of total RNA levels and western blotting for DDX5, hnRNP A2/B1, ribosomal proteins RPLP0 (large subunit) and RPS5 (small subunit). Unseparated heavy complexes accumulated at the bottom of the gradient (heavy fraction 13). One representative blot of three similar experiments is shown. (K) Fractions were measured for the relative abundance of *Mbp*, *Cnp* and *Pgk1* mRNA by qRT-PCR in comparison to the input sample (n=3, mean±s.e.m.). Arrows indicate ribosomal fractions with enriched *Mbp* mRNA levels.

Journal of Cell Science (2018) 131, jcs204750. doi:10.1242/jcs.204750

of adherent cells was carried out after 3 days in vitro (DIV), when endogenous DDX5 levels had decreased (Fig. 3A). Contrary to the knockdown experiments, $DDX5^{WT}$ overexpression in primary oligodendrocytes significantly reduced levels of MBP protein (Fig. 4B,C), without changing the corresponding RNA levels (Fig. 4D), again pointing to post-transcriptional regulatory mechanisms. Overexpression of mutant $DDX5^{K144N}$ did not reduce MBP protein levels (Fig. 4C, MBP), indicating that $DDX5^{WT}$ helicase activity was instrumental for the observed alterations. Interestingly, levels of CNP were also affected (Fig. 4C, CNP), but the decrease in both conditions ($DDX5^{WT}$ and $DDX5^{K144N}$) suggests a mechanistically different explanation that is independent of DDX5 helicase activity. Taken together, our results suggest that DDX5 inhibits MBP protein synthesis via post-transcriptional mechanisms mediated at least in part by its helicase activity.

DDX5 is involved in the regulation of MBP isoform abundance

DDX5 has been described as a factor regulating pre-mRNA splicing (Dardenne et al., 2014). Indeed, when we knocked down DDX5 in primary oligodendrocytes and analyzed MBP expression by western blotting, we not only found increased amounts of total MBP (Fig. 3B) but also a shift in the relative proportions of MBP isoforms (Fig. 5A,B). Six classical MBP isoforms generated by alternative splicing have been so far identified in mouse oligodendrocytes, three containing exon 2 and three lacking exon 2 (Fig. 5E). Isoform-specific densitometric analysis of western blots suggested that DDX5 knockdown primarily increased the abundance of exon 2-positive 21.5 kDa and 17 kDa isoforms, while the exon 2-negative 14 kDa isoform appeared unaffected (Fig. 5A). Moreover, isoform-specific mRNA analysis of DDX5-deficient primary oligodendrocytes by qRT-PCR also revealed an increased ratio of exon 2-positive to exon 2-negative isoforms at the mRNA level (Fig. 5B). To determine if changes in *Mbp* mRNA isoform ratios were dependent on DDX5 helicase activity, we transfected Oli-*neu* cells with $DDX5^{WT}$ or the corresponding helicase-inactive mutant $DDX5^{K144N}$ (Fig. 5C). Isoform analysis by qRT-PCR revealed that compared with DDX5 knockdown, DDX5 (WT or K114N) overexpression led to the opposite effect: a decrease in the ratio of exon 2-positive versus exon 2-negative isoforms and this was independent of DDX5 helicase activity (Fig. 5D). In summary, these results indicate an involvement of DDX5 in the regulation of alternative splicing of *Mbp*, leading to inclusion of exon 2 into the mature mRNA in the absence of DDX5 (Fig. 5E).

DDX5 knockdown affects formation of MBP-positive processes along nanofibers

To further assess the role of DDX5 during differentiation and initial steps of myelination, we analyzed MBP expression in siRNA-treated primary oligodendrocytes associating with electrospun polycaprolactone (PCL) nanofibers. Cell culture inserts with aligned nanofibers of 700 nm diameter were used to provide an artificial scaffold physically mimicking white matter axonal processes. Recent reports showed that oligodendrocytes sense, contact and enwrap nanofibers (Lee et al., 2012) and such scaffolds serve as a method to study the initial steps of OL-intrinsic myelination independently of axonal signals (Bechler et al., 2015).

We isolated primary OPCs by sorting with NG2-coupled beads and allowed them to differentiate into mature oligodendrocytes on nanofiber inserts for 5 days. Single-molecule FISH for *Mbp* mRNA and combined immunocytochemistry of DDX5 revealed a granular distribution of DDX5 in processes of mature oligodendrocytes (Fig. S4). DDX5 also overlapped with the *Mbp* mRNA signals in the processes along the nanofiber matrix (Fig. S4B), which was similar to the distribution in more immature cells. Subsequently, we analyzed oligodendrocytes cell numbers and MBP expression in response to knockdown of DDX5 or hnRNP A2/B1 (as a direct comparison, Fig. 6A). Western blot analysis confirmed an efficient knockdown of DDX5 with the resulting increase of MBP protein and, as expected, a decrease in MBP protein levels after hnRNP A2/B1 reduction was observed (Fig. 6B). Immunostaining for Olig2, MBP and DAPI revealed a decrease in total cell numbers of $Olig2^{+}$ cells in nanofiber cultures treated with DDX5 or A2/B1 siRNA compared with control siRNA-treated cells (Fig. 6C,F). However, the number of $Olig2^{+}$ cells expressing MBP was increased in response to DDX5 knockdown compared with levels in both the hnRNP A2/B1 knockdown and the control (Fig. 6G).

We analyzed how knockdown of DDX5 or hnRNP A2/B1 affects the distribution of MBP^{+} processes in the cells associated with the nanofiber matrix. OL processes extended along the nanofibers and intensely expressed MBP protein, indicating maturation of the cells. Membrane sheet extension was clearly visible but we did not find multilamellar wrapping and myelin-like segments on the nanofibers at DIV 5. We measured the length of the cellular MBP^{+} extensions in parallel to the nanofiber orientation (Fig. 6D) and found an increased longitudinal distribution of MBP after DDX5 knockdown, whereas knockdown of hnRNP A2/B1 reduced the extension of MBP^{+} processes along the nanofibers (Fig. 6D,E,H). Taken together, DDX5 knockdown in these conditions reduces the number of oligodendroglial lineage cells but increases MBP expression and extension of MBP^{+} processes along the nanofiber matrix.

DISCUSSION

The spatiotemporal expression of MBP is a key step during oligodendroglial maturation and myelin biogenesis (Aggarwal et al., 2013; Harauz and Boggs, 2013) and the transition from OPCs to mature oligodendrocytes, including the upregulation of MBP sets a critical time window for initial steps of myelination and remyelination (Franklin and Goldman, 2015; Kuhlmann et al., 2008; Miron et al., 2011). In cultured oligodendrocytes, MBP instructs the polarization and composition of sheet-like membrane extensions (Fitzner et al., 2006) and such multipolar pre-myelinating oligodendrocytes served as a model for visualizing *Mbp* mRNA molecules with single-molecule resolution here.

DDX5 as a component of heterogeneous *Mbp* mRNA-containing complexes

In a search for components of *Mbp* mRNA-associated ribonucleoprotein complexes, we identified the DEAD-box RNA helicase DDX5. It is a strikingly multifunctional protein involved in various aspects of RNA metabolism and an important target in cancer research. In our cultured primary oligodendrocytes, DDX5 expression decreases during differentiation from proliferative OPCs to post-mitotic oligodendrocytes. At the subcellular level, the predominant nuclear localization of DDX5 in oligodendrocytes matches its proposed functions in transcriptional co-regulation (Fuller-Pace, 2013), mRNA splicing (Camats et al., 2008; Dardenne et al., 2014; Kar et al., 2011) or miRNA processing (Hong et al., 2013; Suzuki et al., 2009; Wang et al., 2012).

DDX5 has previously been suggested to be a component of RNA granules in the rodent brain (Elvira et al., 2006; Kanai et al., 2004). In accordance with this, we additionally observed DDX5 to

Journal of Cell Science (2018) 131, jcs204750. doi:10.1242/jcs.204750

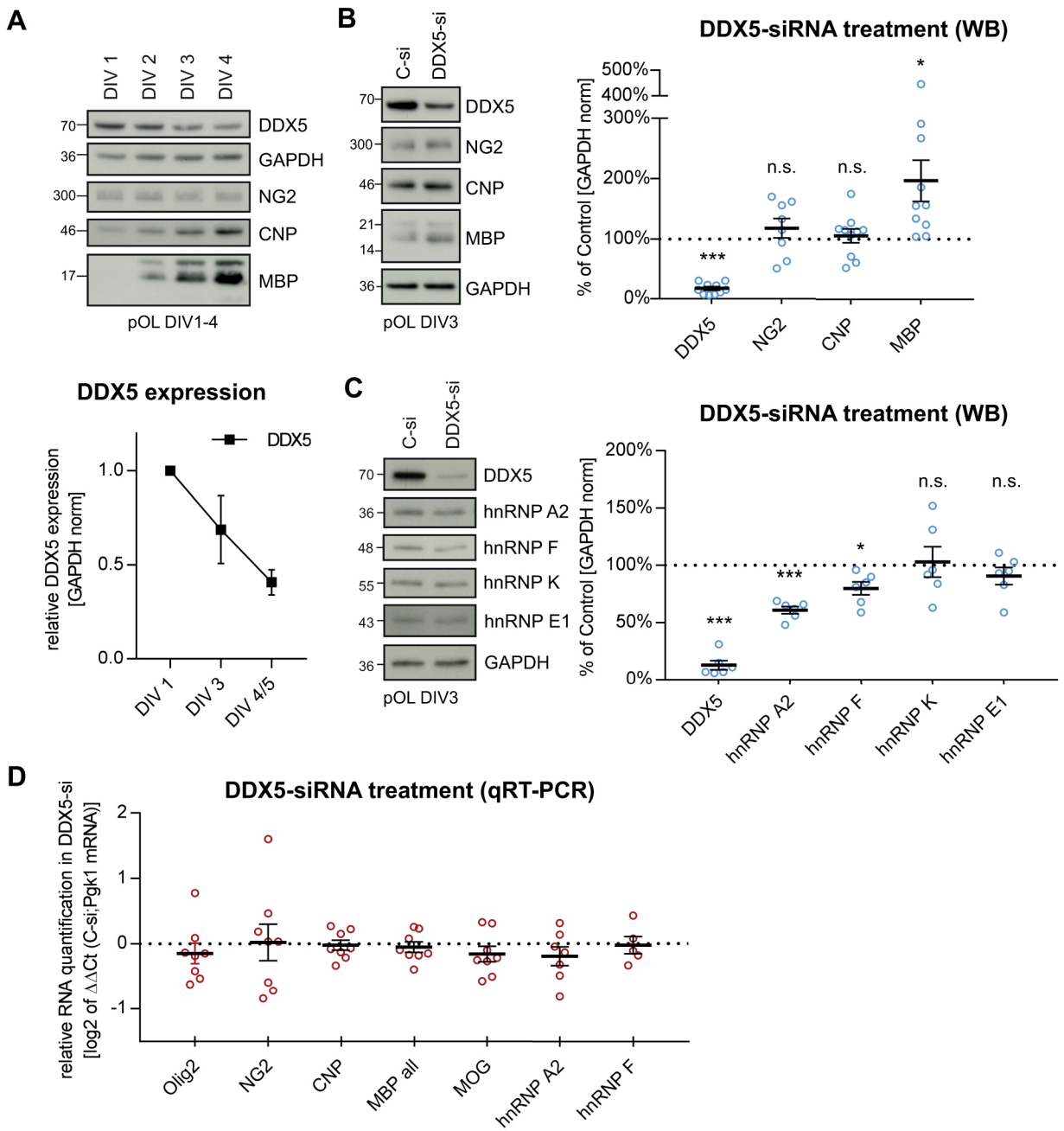

Fig. 3. DDX5 post-transcriptionally contributes to the regulation of MBP levels. (A) Primary mouse oligodendrocytes (embryonic) were analyzed by western blotting (top) at different differentiation stages (DIV 1-4). Note the increasing expression of myelin proteins (CNP, MBP) in the course of the differentiation. Expression of DDX5 decreases during oligodendroglial development. DDX5 protein levels were normalized to GAPDH expression and presented relative to DIV 1 (bottom; *n*=3, mean±s.e.m.). (B,C) Primary mouse oligodendrocytes (embryonic) were treated with control or DDX5 siRNA and analyzed by western blotting after 3 DIV and analyzed for (B) myelin proteins and (C) *Mbp* mRNA-associated RBPs. Note that the blot shown in C was reprobed for individual MBP proteins in Fig. 5A. Densitometrically quantified protein levels were normalized to GAPDH expression and presented relative to C-si treatment (control). Individual data points are displayed as blue circles. Black lines represent the mean±s.e.m. (*n*=6-10); **P*<0.05, ****P*<0.001 (one-sample *t*-test, two-tailed). Total MBP protein levels are selectively elevated whereas hnRNPs A2/B1 and F are reduced upon DDX5 knockdown. (D) Corresponding total RNA was extracted from cells used in B and C and mRNA levels were determined by qRT-PCR. Levels were related to control siRNA-treated cells and the abundance of *Pgk1* mRNA. Individual data points are displayed as red circles. Black lines represent mean±s.e.m.; *n*=5-8.

localize to cytoplasmic granular puncta within the oligodendrocyte soma and processes. DDX5 immunoprecipitations enriched *Mbp* mRNA compared with control mRNAs and smFISH for *Mbp* transcripts and combined immunocytochemistry revealed an overlap of DDX5 protein with *Mbp* mRNA signals, which appeared to be more prominent than that of hnRNP A2/B1 with *Mbp* mRNA. Only a subpopulation of *Mbp* mRNA-positive puncta showed an overlap with both DDX5 and hnRNP A2/B1. Unexpectedly, we could not reliably detect hnRNP A2/B1 in DDX5 immunoprecipitations, although these were enriched in *Mbp* mRNA and we initially identified DDX5 as a protein associated with hnRNP A2/B1 immunoprecipitates. However, most of the few *Mbp* mRNA/hnRNP A2/B1 double-positive puncta also overlapped with DDX5 protein staining or appeared to

Journal of Cell Science (2018) 131, jcs204750. doi:10.1242/jcs.204750

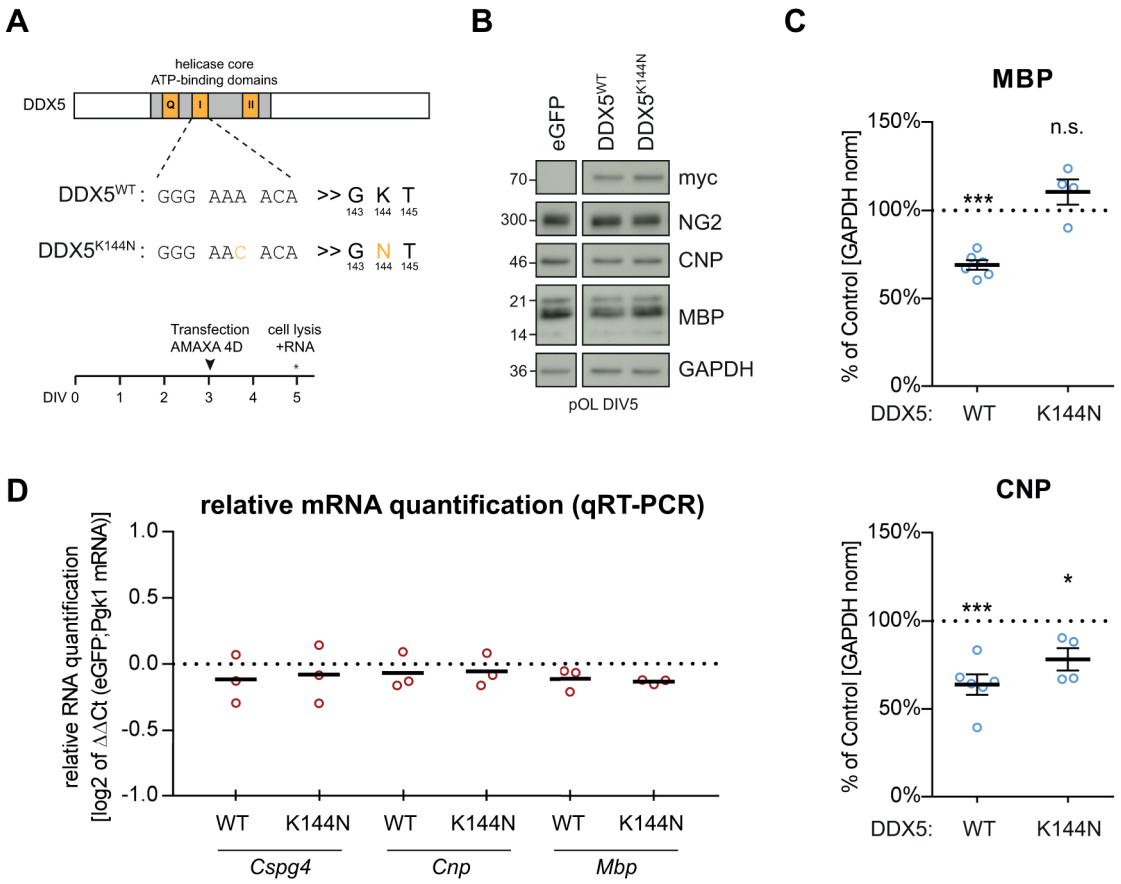

Fig. 4. The helicase activity of DDX5 is required for post-transcriptional regulation of MBP. (A) Schematic representation of the K144N mutation in the resulting myc-tagged DDX5 polypeptide in order to disrupt ATP-binding and the helicase activity and the experimental time course. (B) Primary mouse oligodendrocytes (embryonic) were transfected with DDX5-myc, its helicase-inactive mutant DDX5^{K144N}-myc or eGFP control plasmids at DIV 3. Expression of CNP and MBP was analyzed after 2 days in culture by western blotting. DDX5 overexpression was monitored with myc-specific antibodies and GAPDH served as loading control. (C) Quantification of western blot signals shows that DDX5^{WT} overexpression reduced levels of MBP and CNP dependent on its helicase activity whereas DDX5^{K144N} did not alter MBP levels. Individual data points are displayed as blue circles. Black lines represent the mean±s.e.m. (n=4-6); *P<0.05, ***P<0.001 (one-way ANOVA followed by a Dunnett's post-test). (D) Corresponding total RNA was extracted from cells used in B and C, and mRNA levels were determined by qRT-PCR. Levels were related to control siRNA-treated cells and the abundance of *Pgk1* mRNA. Individual data points are displayed as red circles. Black lines represent the mean from 3 independent experiments.

be in close proximity, which may explain our initial identification of DDX5 in the mass spectrometric analysis. DDX5 and hnRNP A2/B1 thus both interact with *Mbp* mRNA but our results suggest an underestimated heterogeneity in *Mbp* mRNA-associated complexes which might depend on the time point, the cellular microenvironment or different intrinsic oligodendrocyte identities (Bechler et al., 2015).

Multiplexing of A2RE-containing transcripts has been described in neurons (Gao et al., 2008), and recently, more than 500 mRNA targets for hnRNPA2/B1 have been mapped by iCLIP (individual-nucleotide resolution crosslinking and immunoprecipitation) in the CNS (Martinez et al., 2016). In oligodendrocytes, multiplexing has not been elucidated in detail, although *Mopb* and other mRNAs have also been suggested to be regulated via the A2RE pathway (Barbarese et al., 1999; Schafer et al., 2016) and a large number of mRNAs have been recently found in myelin preparations (Thakurela et al., 2016). Deciphering these heterogeneous populations of *Mbp* RNA granules remains a challenging task and high-resolution spatiotemporal analysis of *Mbp* mRNA and associated factors *in situ* will be necessary to further elucidate the heterogeneity of *Mbp* RNP complexes and to better understand post-transcriptional regulation mechanisms during oligodendrocyte maturation.

DDX5 mediates inhibition of MBP protein synthesis by post-transcriptional mechanisms

The phase transition of MBP molecules during myelin membrane compaction and also potential signaling functions of soluble MBP molecules are dependent on the local MBP protein concentration (Aggarwal et al., 2013; Harauz and Boggs, 2013). Furthermore, proper assembly of the myelin sheath containing compact and non-compact areas involves a coordinated interplay of actin cytoskeleton dynamics and the presence of MBP (Zuchero et al., 2015; Snaidero et al., 2017). Therefore, robust translational control of *Mbp* mRNA needs to be guaranteed during early oligodendrocyte maturation, to avoid premature onset of MBP production.

At early stages of differentiation, primary oligodendrocytes contain considerable numbers of *Mbp* transcripts but only weak signals for MBP protein could be detected and DDX5 expression inversely correlates with upregulation of MBP protein synthesis during differentiation. RNAi-mediated knockdown of DDX5 increased expression of MBP while overexpression of DDX5 in maturing oligodendrocytes led to a decrease in MBP protein without affecting mRNA levels, rendering DDX5 as a post-transcriptional inhibitor of MBP protein synthesis. In density gradients of oligodendroglial cytoplasmic extracts we could detect DDX5 in

Journal of Cell Science (2018) 131, jcs204750. doi:10.1242/jcs.204750

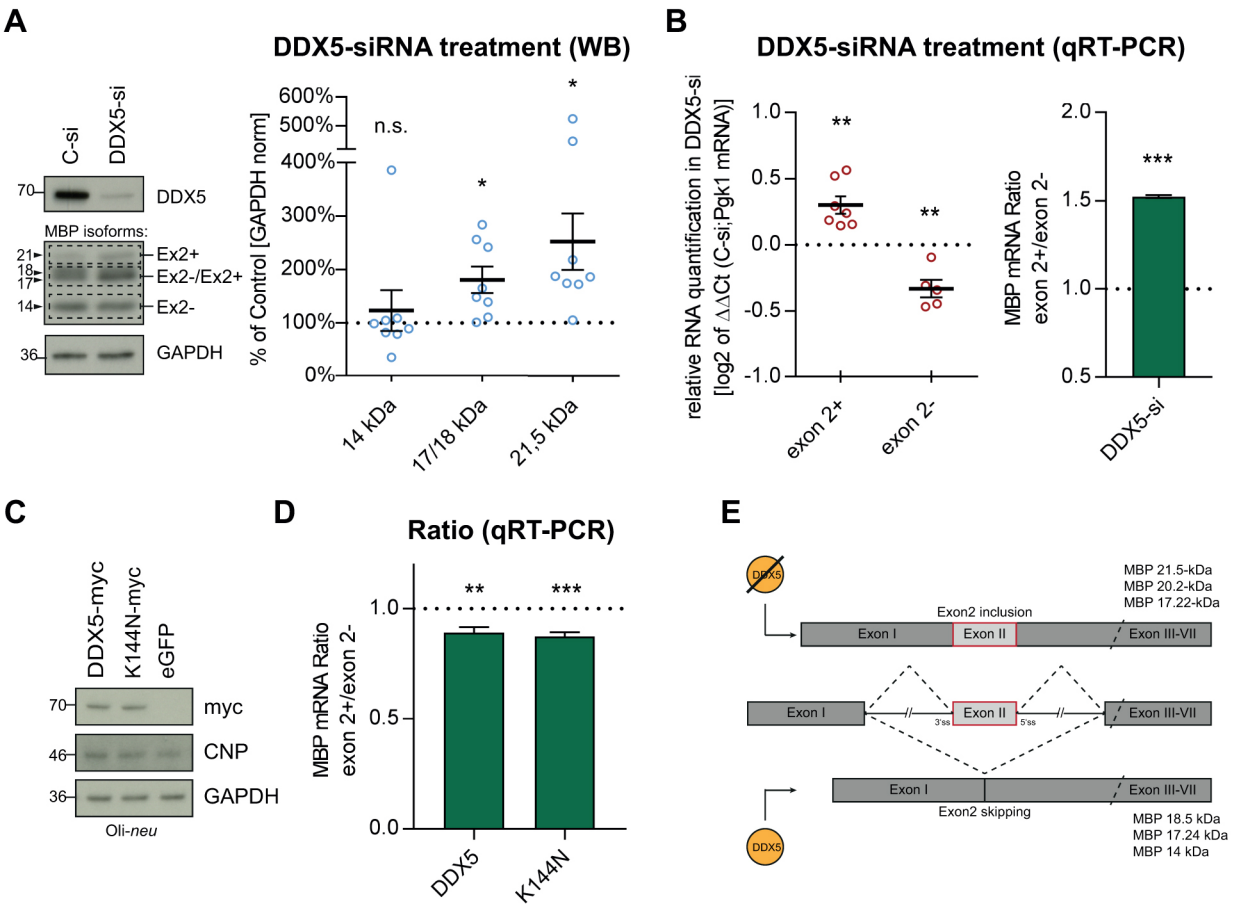

Fig. 5. Variations in MBP isoforms upon DDX5 manipulation. (A) Western blots of siRNA-treated primary mouse oligodendrocytes from Fig. 3B-D were additionally analyzed in respect to individual MBP isoforms. The MBP isoforms exhibit a similar mobility in SDS-PAGE and we were able to discriminate between a 14 kDa band lacking exon 2, a 21 kDa band containing exon 2 and a 17-18 kDa doublet consisting of both exon 2-negative and -positive isoforms. Note the exclusive increase in signals containing exon 2-positive isoforms (MBP 17 and 21). Densitometrically quantified protein levels were normalized to GAPDH expression and presented relative to C-si treatment (control). Individual data points are displayed as blue circles. Black lines represent the mean±s.e.m. from 8 independent experiments; n.s. not significant, **P*<0.05 (one-sample *t*-test). (B) Total RNA from Fig. 3D was analyzed for *Mbp* exon 2-negative and exon 2-positive specific mRNA levels by qRT-PCR. Levels were related to control siRNA-treated cells and the abundance of *Pgk1* mRNA. Additionally, the ratio between exon 2-positive and exon 2-negative isoforms is displayed in the right panel. Individual data points are displayed as red circles. Data represent the mean±s.e.m. from 5 independent experiments; ***P*<0.01, ****P*<0.001 (one sample *t*-test, two-tailed). (C) Overexpression of myc-tagged DDX5 or its helicase-inactive mutant DDX5^{K144N} was carried out in Oli-*neu* cells and was monitored using myc-specific antibodies. (D) Corresponding total RNA was extracted from cells in C and relative expression of individual *Mbp* mRNA isoforms was assessed by qRT-PCR. mRNA levels were related to control siRNA-treated cells and *Pgk1* mRNA and the ratio of *Mbp* exon 2-positive to exon 2-negative isoforms is displayed as mean±s.e.m. from 5 independent experiments; ***P*<0.01, ****P*<0.001 (one-way ANOVA followed by a Dunnett's post-test). (E) Schematic representation of DDX5-dependent *Mbp* exon 2 inclusion or skipping.

fractions containing ribosomal subunits and *Mbp* mRNA, supporting a role for DDX5 in translational regulation of MBP. Together with the finding that other markers of oligodendrocyte differentiation and the number of MBP$^+$ cells were not altered at DIV3, this suggests that DDX5 knockdown does not primarily affect the general timing of oligodendrocyte maturation but rather acts specifically on MBP during this early differentiation period.

However, prolonged knockdown of DDX5 led to diminished numbers of oligodendroglial lineage cells in maturing oligodendrocytes cultured for 5 days on aligned nanofiber scaffolds (mimicking axonal white matter tracts) although MBP expression was upregulated. Thus, a long-term reduction of DDX5 levels might impair general oligodendroglial development and/or survival. Furthermore, extension of MBP$^+$ processes along the nanofibers was enhanced by DDX5 knockdown (in contrast to knockdown of hnRNP A2/B1, which has the opposite effect), suggesting that DDX5 might be involved in the intrinsic regulation of initial steps of axon ensheathment. Accordingly, the presence of DDX5-containing *Mbp* mRNA granules in mature oligodendrocyte processes elongated on the nanofiber matrix indicates a role in the spatiotemporal regulation of MBP expression that is not restricted to immature oligodendrocytes.

Cytoplasmic RNA granules are dynamic RNP complexes that exchange factors to modulate the mRNP function according to the cellular state (Anderson and Kedersha, 2009; Buchan, 2014). The respective mRNP composition depends on sequence-specific mRNA secondary structures as well as the local RBP availability and modification in the developing cell. As an RNA helicase, DDX5 is capable of remodeling *Mbp* mRNA secondary structures, potentially interfering directly with translational activation or the association of silencing co-factors. In agreement with this concept, DDX5 and its yeast orthologue Dbp1 have been shown to modulate the assembly of RNP complexes (Camats et al., 2008; Kar et al., 2011; Ma et al., 2013). In our experiments, overexpression of the helicase-dead DDX5^{K144N} mutant did not decrease MBP levels in contrast to wild-type DDX5, suggesting that the DDX5 helicase

Journal of Cell Science (2018) 131, jcs204750. doi:10.1242/jcs.204750

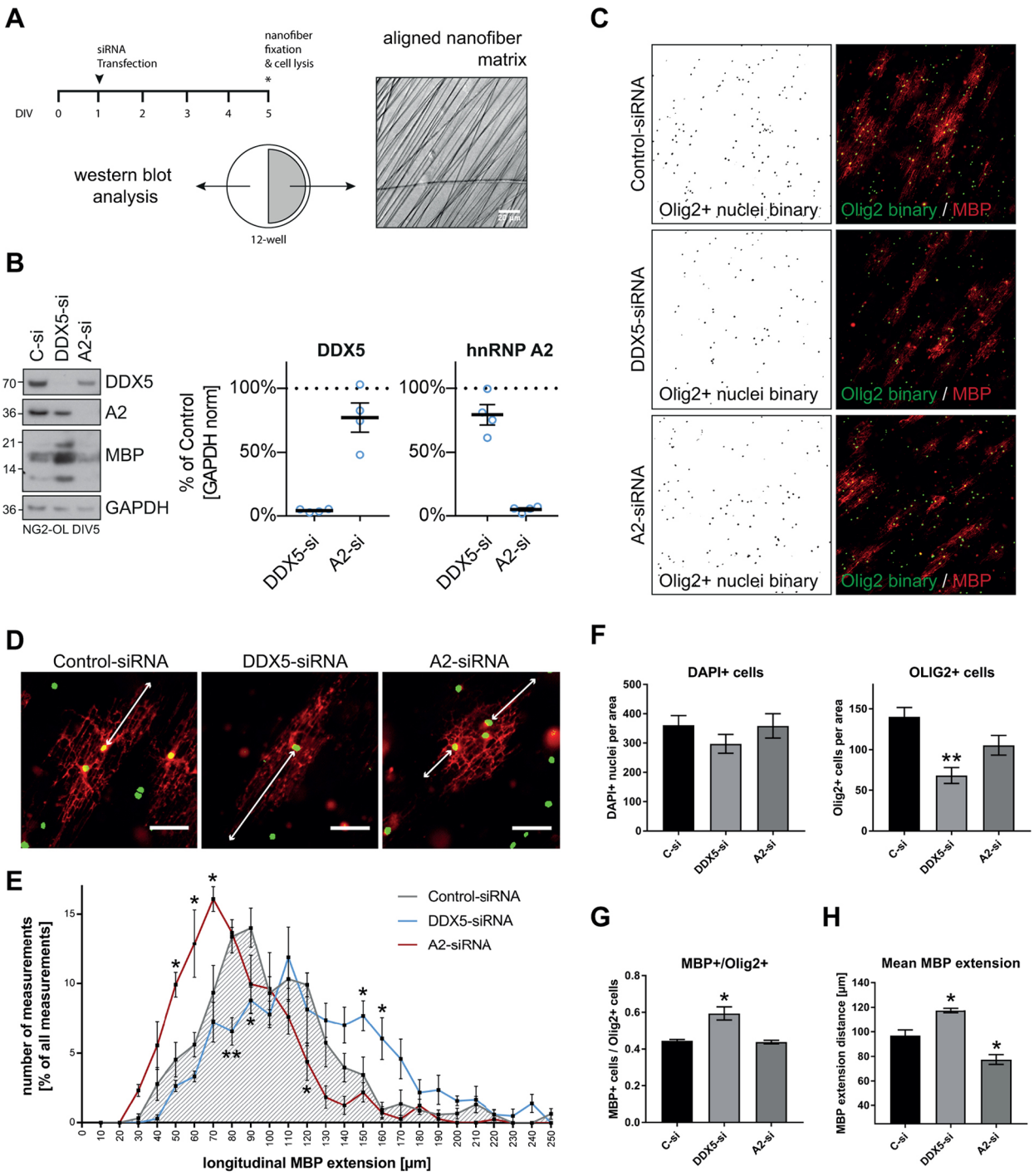

Fig. 6. Knockdown of DDX5 affects nanofiber-associated mature oligodendrocytes. (A) NG2$^+$ OPCs were isolated by MACS sorting and seeded in 12-well plates containing half of a nanofiber matrix insert, with half of the well lacking the insert for western blot analysis of plated cells. Cells were treated with control, DDX5 or hnRNP A2/B1 siRNA and analyzed by western blotting or immunocytochemistry after 5 DIV. Four independent experiments were performed for each condition (n=4). (B) Western blot and densitometric quantification of DDX5 and hnRNP A2/B1 protein levels. Signals were normalized to GAPDH expression and presented relative to C-si treatment (control). Individual data points are displayed as blue circles. Black lines represent the mean±s.e.m. from 4 independent experiments. (C-H) Immunocytochemistry on nanofiber inserts and subsequent image analysis. (C) Cells on nanofiber inserts were stained for Olig2, MBP and DAPI. Only Olig2$^+$ and DAPI$^+$ double-positive nuclei were considered as Olig2$^+$ oligodendrocytes, counted as binary images and displayed in combination with MBP. Images were taken for each experimental condition and were analyzed by cell counting (8 images per condition) or measurement of longitudinal MBP extension (at least 60-130 measurements per condition). (D) To obtain the longitudinal MBP distribution on the nanofibers, the maximal distance of the cellular MBP signal from the cell nucleus was measured in parallel to the nanofiber orientation and compared between the siRNA treatments. Representative measurements are shown as white arrows. Scale bars: 50 µm. (E) Normalized number of segments of indicated length are plotted in the normalized histogram. Note the shift towards shorter extensions in A2/B1 siRNA treated or longer extensions in DDX5 siRNA-treated cells. (F-H) Statistical analysis of cell counting and mean MBP extension. (F) Cells were counted with ImageJ and total cell numbers for DAPI$^+$ or Olig2$^+$ cells are shown per area for each image. (G) The ratio of MBP$^+$/Olig2$^+$ cells is increased after 5 days of DDX5 knockdown. (H) MBP extension distance is shown as a mean±s.e.m. of all measurements per condition according to the experiments in D and E. All data are mean of four independent experiments (n=4). *P<0.05, **P<0.01 (two-tailed Student's t-test, each related to C-si).

Journal of Cell Science (2018) 131, jcs204750. doi:10.1242/jcs.204750

activity is indeed involved in the translational regulation of *Mbp* mRNA. In a possible scenario, DDX5 might facilitate binding of inhibitory factors such as hnRNP E1 (PCBP1) (Kosturko et al., 2006; Torvund-Jensen et al., 2014) or Argonaute-2 complexes (Müller et al., 2015; Wang et al., 2010), including small non-coding RNA-715 (Bauer et al., 2012) to *Mbp* mRNA. In line with this, a cytoplasmic interaction of DDX5 and Argonaute-2 has been postulated before in HeLa cells (Geissler et al., 2013) and DDX5 has been described as specifically unwinding and loading let-7a miRNA into functional RNA silencing complexes (Salzman et al., 2007). On the other hand, DDX5 might prevent binding of stimulating factors such as TOG (Francone et al., 2007; Maggipinto et al., 2017) or hnRNP K (Laursen et al., 2011; Torvund-Jensen et al., 2014) interfering with proper assembly of translationally silent transport granules, remodeling towards translational activation.

Secondary post-transcriptional effects influencing the MBP synthesis pathway

DEAD-box RNA helicases have been described as multifunctional proteins (Linder and Jankowsky, 2011) and despite the fact that DDX5 is present in *Mbp* mRNA granules, this does not exclude a potential role in translational repression of *Mbp* via additional secondary effects. In our experiments, we found that cytoplasmic levels of hnRNP A2/B1 and hnRNP F were reduced post-transcriptionally in response to DDX5 knockdown. However, alterations in the levels of hnRNP A2/B1 and hnRNP F have been reported to lead to a reduction of MBP protein (Laursen et al., 2011; Torvund-Jensen et al., 2014; White et al., 2012) in contrast to the increase that our experiments show. Hence, in the present context it remains unclear, if and how these RBPs contributed to the observed effect on MBP. Finally, DDX5 overexpression in our experiments also altered levels of selective myelin proteins (e.g. CNP) post-transcriptionally, but independently of its helicase activity. Specific insights into these potential regulatory mechanisms remain elusive but this would be in line with an assumed multifunctionality of DDX5 in oligodendroglial cells, including processing of selected pri-miRNA as a constituent of nuclear DROSHA (Hong et al., 2013; Suzuki et al., 2009).

A role of DDX5 in alternative splicing of *Mbp* isoforms in immature oligodendrocytes

A functional consequence of our DDX5 depletion in primary oligodendrocytes was the increased expression of MBP exon 2-containing isoforms. The inverse correlation of *Mbp* exon 2-negative versus exon 2-positive isoform levels as a result of DDX5 manipulation suggests a regulatory effect on alternative splicing, rather than an altered stability of the different individual transcripts. In contrast to the effect of DDX5 at the translational level, this appeared to be independent of its helicase activity. DDX5 has previously been implicated in the regulation of alternative splicing of diverse targets using different mechanisms (Camats et al., 2008; Kar et al., 2011; Lin et al., 2005), and DDX5 and DDX17 have been identified as ‘master orchestrators’ of switching between splicing programs during cell differentiation (Dardenne et al., 2014), suggesting that *Mbp* mRNA might not be the only splicing target of DDX5 in oligodendrocytes.

Primary *Mbp* mRNA transcripts are alternatively spliced at exon 2 and exon 5/6, whereas functional differences have mainly been postulated depending on the presence or absence of exon 2, which encodes a non-traditional PY nuclear localization signal (Smith et al., 2012) with the potential to change MBP protein localization and functions (Ozgen et al., 2014; Pedraza et al., 1997; Smith et al., 2013). Although several factors, including Quaking RBPs (Larocque et al., 2002; Wu et al., 2002), Fyn kinase (Lu et al., 2005) or DDX54 (Ueki et al., 2012; Zhan et al., 2013) have been shown to affect the abundance of MBP exon 2-positive versus exon 2-negative isoforms, mechanistic insights into the regulation of this phenomenon remain to be elucidated. Interestingly, knockdown of the factors mentioned above also severely impact myelination in the CNS. Exon 2-positive isoforms are expressed early in oligodendrocyte differentiation (Barbarese et al., 1978) and furthermore, are upregulated during active phases of chronic relapsing autoimmune disease in experimental allergic encephalomyelitis (EAE) (Nagasato et al., 1997) and remyelination in chronic human multiple sclerosis lesions (Capello et al., 1997). Consequently, MBP exon 2-containing isoforms may influence early oligodendrocyte maturation and remyelination independently of a classical function in myelin membrane compaction.

Converging roads towards MBP expression

Our work reported here suggests that DDX5 is present in subpopulations of *Mbp* mRNA-containing complexes and mediates alternative splicing and post-transcriptional repression of MBP synthesis in pre-myelinating oligodendrocytes. In previous work, DDX5 functioned at different levels of gene expression, acting on alternative splicing and miRNA processing or transcription in concert (Dardenne et al., 2014; Samaan et al., 2014). An emerging concept is the connection of nuclear RNA modification events with the cytoplasmic mRNA fate (Haimovich et al., 2013; Moore and Proudfoot, 2009) and the splicing-dependent deposition of DDX5 on transcripts (Merz et al., 2007) would serve as an exciting hypothesis suggesting that DDX5 is involved in bridging these processes also in oligodendrocytes. Interestingly, *Mbp* exon 2-containing transcripts, bearing a 3′UTR common to all *Mbp* isoforms, show distinct perinuclear localization patterns that correlate with the localization of exon 2-containing proteins (de Vries et al., 1997). Decoration of *Mbp* mRNA with selected factors during alternative splicing in response to DDX5 thereby might already predetermine the cytoplasmic fate of the mRNA.

Interestingly, as a potential target in cancer therapy, DDX5 can be directly targeted by compounds already tested in humans, such as the antioxidant resveratrol (Taniguchi et al., 2016), the active component of green tea epigallocatechin gallate (ECGC) (Tanaka et al., 2011) or the synthetic drug Supinoxin/RX-5902 (Kost et al., 2015). It is conceivable that oligodendrocyte-specific targeting of DDX5 could facilitate *Mbp* translation *in vivo*, aiding myelination or remyelination in the context of white matter disease.

MATERIALS AND METHODS

Oligodendroglial cell culture

C57BL/6-N wild-type mice (*Mus musculus*) were obtained from the Translational Animal Research Center (TARC, Mainz) and experiments were carried out in accordance with the animal policies of the University of Mainz. Embryonic cultures were prepared as described (Gonsior et al., 2014) by shaking off primary neuron-depleted oligodendrocytes from a feeder astrocyte cell layer and cultured in B27 medium supplemented with 1% horse serum (HS), PDGF-AA (10 ng/ml, PeproTech) and bFGF (5 ng/ml, PeproTech). Alternatively, primary oligodendroglial cells were isolated with anti-AN2/NG2 or anti-O4 microbeads (Miltenyi) from P7-P9 mouse brains using the NeuroMACS Neural Tissue Dissociation Kit (P) and subsequent magnetic-activated cell sorting (MACS) cell separation procedure according to the manufacturer’s recommendations (Miltenyi).

Journal of Cell Science (2018) 131, jcs204750. doi:10.1242/jcs.204750

NG2-sorted cells were cultured in OPC medium (MACS Neuro medium, Miltenyi) supplemented with 1× NeuroBrew21 (Miltenyi), penicillin-streptomycin (100 U/ml, Life Technologies), L-glutamine (2 mM, Life Technologies), Forskolin (4.2 µg/ml, Sigma), CNTF (10 ng/ml), PDGF (10 ng/ml, PeproTech) and NT-3 (1 ng/ml, PeproTech). O4-sorted cells were kept in OL medium (MACS Neuro medium, Miltenyi) supplemented with 1× NeuroBrew21 (Miltenyi), penicillin-streptomycin (100 U/ml, Life Technologies), L-glutamine (2 mM, Life Technologies), bFGF (5 ng/ml, PeproTech) and PDGF-AA (10 ng/ml, PeproTech). Primary cells were plated in appropriate poly-L-lysine (PLL)-coated culture dishes or Neuroclean 11 mm coverslips (Prime Glass) and cells were analyzed after 1-5 DIV. The Oli-*neu* cell line (Jung et al., 1995) was cultured in Sato Medium supplemented with 1% HS on PLL-coated cell culture vessels as described (Gonsior et al., 2014) and tested for contamination regularly. Oli-*neu* cells were induced to differentiate by daily addition of 1 mM dibutyryl cyclic AMP (dbcAMP) to the cell culture medium.

Plasmids, siRNA and transfection

To generate myc-His-tagged DDX5 expression constructs, the reverse transcribed murine DDX5 CDS was cloned into the pcDNA4/TO/myc-His backbone using restriction sites *Bam*HI and *Xba*I. The DDX5^{K144N} mutation was inserted using the Quikchange II Site-directed Mutagenesis Kit (Agilent) using the following primers: forward, 5′-GCTCAGACTGGATCTGGGAACACATTATCTTATTTGCTGCC-3′ and reverse, 5′-GGCAGCAAATAAGATAATGTGTTCCCAGATCCAGTCTGAGC-3′. For control transfections, the eGFP-C3 vector (Clontech) was utilized. Fyn constructs were generated before (White et al., 2012). Transfection of 10 µg plasmid DNA into adherent primary oligodendrocytes DIV 3 was achieved using the AMAXA 4D-Nucleofector Y Unit (program ED-158) with the Amaxa 4D-Nucleofector basic protocol for mammalian neural cells (Lonza). Adherent Oli-*neu* cells (6-well) were transfected with 2 µg of plasmid DNA using FuGene HD in a 4:2 ratio (Promega). RNAi transfection of primary oligodendrocytes (cell suspension after Oligo shake) or Oli-*neu* cell suspension was carried out using DDX5 siRNA (DDX5-si, siGENOME SMARTpool DDX5 siRNA #M-06-533-01-0005, Thermo Fisher Scientific), hnRNP A2/B1 (A2-si, siGENOME SMARTpool Hnrnpa2b1 siRNA #M-040194-01-0005) or non-targeting control siRNA (C-si, target sequence 5′-AATTCTCCGAACGTGTCACGT-3′, Qiagen) in the AMAXA Nucleofector II device (program O-005) with the Amaxa Basic Nucleofector Kit for Primary Neurons according to the manufacturer's instructions (Lonza).

Primary antibodies

Antibodies used on western blots (WB) or in immunocytochemistry (ICC) were: mouse anti-hnRNP A2/B1 (1:500 WB or 1:100 ICC, clone EF67, gift from Dr William Rigby, Dartmouth Medical School, Lebanon, NH, USA), mouse anti-hnRNP A2/B1 (1:500 WB, R4653, Sigma), rabbit anti-DDX5 (1:3000 WB or 1:200 ICC, A300-523A, Bethyl), mouse anti-CNP (1:500 WB or 1:200 ICC, 11-5B, Sigma-Aldrich), rat anti-MBP (1:500 WB or 1:500 ICC, MCA409S, Serotec), rabbit anti-GAPDH (1:3000 WB, A300-641A, Bethyl), rabbit anti-hnRNP F (1:1500 WB, ab50982, Abcam), mouse anti-hnRNP K (1:1000 WB, ab23644, Abcam), goat anti-hnRNP E1 (1:100 WB, T18, sc16504, Santa Cruz), rabbit anti-RPLP0 (1:5000 WB, ab101279, Abcam), rabbit anti-RPS5 (1:500 WB, ab58345, Abcam), rat anti-NG2 (1:200 WB or 1:20 ICC, Prof. Jacqueline Trotter, JGU Mainz, Germany), mouse anti-myc-tag (1:500 WB, #M5546, Sigma), mouse anti-phospho-tyrosine (1:500 WB, clone 4G10, Merck Millipore), rabbit anti-Src[PY418] (1:500 WB, 44660G, Invitrogen) and rabbit anti-Olig2 (1:1000 ICC, AB9610, Merck Millipore).

Cell lysis, SDS-PAGE and western blotting

Primary oligodendrocytes or Oli-*neu* cells were scraped and lysed on ice using modified RIPA buffer [50 mM Tris-HCl, pH 7.4, 150 mM NaCl, 1 mM EDTA, 1% (v/v) NP-40 Substitute, Halt Protease and Phosphatase Inhibitor Cocktails (Thermo Fisher)] and post-nuclear supernatant (PNS) was collected after centrifugation at 1000 ***g*** for 10 min. Proteins were resolved on 12% polyacrylamide gels in a Mini PROTEAN 3 system (Bio-Rad) or Novex NuPAGE SDS-PAGE 4-12% Bis-Tris gradient gels (Thermo Fisher Scientific) and blotted on ethanol-activated PVDF membranes (Roth) using the Mini Trans-Blot Electrophoretic Transfer Cell system (Bio-Rad). Proteins were analyzed with indicated primary antibodies in combination with HRP-conjugated, species-matching secondary antibodies (Dianova). Chemoluminescent signals were detected with ECL Hyperfilms (GE healthcare) using an OptiMax X-Ray film processor, scanned and densitometrically quantified with ImageJ v.1.43.

RNA isolation, cDNA library preparation and qRT-PCR analysis

Total RNA was obtained from crude cell lysates, density gradient fractions or RNA immunoprecipitation (RIP) eluates in Qiazol and isolated with the miRNeasy Mini Kit (Qiagen) including DNase I digestion using an RNase-free DNase Kit (Qiagen). mRNA was reverse transcribed using the Transcriptor First Strand cDNA Synthesis Kit (Roche) using random hexamer primers. Quantitative Real-time PCR was performed on a StepOne Real-Time PCR system (Applied Biosystems) with gene-specific Taqman Gene Expression Assays: *Mbp* all classic isoforms (Mm01262037_m1), *Mbp* exon 2-containing isoforms (Mm01262035_m1), *Mbp* exon 2-lacking isoforms (Mm00521980_m1), *Cnp* (Mm01306640_m1), *Mog* (Mm00447824_m1), *Pgk1* (Mm00435617_m1), *Rn18s* (Mm03928990_g1), *Ng2*/*Cspg4* (Mm00507256_m1), *β-actin* (Mm00607939_s1), *Olig2* (Mm01210556_m1), *hnRNP A2* (Mm01325931_g1), *hnRNP F* (Mm02527919_g1). Relative RNA Quantification (RQ) was done according to ΔΔCt calculation method using *Pgk1* as a reference gene in StepOne v.2.3 (Applied Biosystems).

hnRNP A2/B1 immunoprecipitation screen

Mouse-anti-hnRNP A2/B1 antibody (EF67) was coupled to Protein-G Sepharose beads (GE healthcare) at a ratio of 1:25 in PBS for 2 h on a rotating wheel at 4°C. Oli-*neu* cell PNS was pre-cleared by incubation with Protein-G Sepharose beads overnight at 4°C. For immunoprecipitation, pre-cleared lysates were incubated with the antibody-coupled beads for 4 h on a rotating wheel at 4°C. Beads were washed four times with lysis buffer, once with PBS and proteins were eluted by the addition of 2× SDS sample buffer with 400 mM DTT for 5 min at 90°C. Proteins were separated by SDS-PAGE and subjected to Roti-Blue Coomassie staining (Roth). Selected protein bands were excised from the gel, digested with trypsin (Promega) and analyzed by nanoscale liquid-chromatography mass spectrometry using data-independent acquisition on a Waters Q-TOF Premier mass spectrometer as described (Wigand et al., 2009). Raw data were processed using PLGS 2.5.2 and searched against the Mouse UniProt Database.

DDX5 RNA co-immunoprecipitation (RIP)

Protein-A-coupled Sepharose beads (GE healthcare) were conjugated with rabbit anti-DDX5 antibody (Bethyl) or normal rabbit IgG (Santa Cruz) as a control in PBS for 3 h on a rotating wheel at 4°C. For immunoprecipitation, PNS was prepared from 2-day differentiated Oli-*neu* cells using RIP lysis buffer containing 50 mM Tris-HCl, pH 7.4, 150 mM KCl, 3 mM $MgCl_2$, 1% (v/v) NP-40 Substitute, Halt Protease and Phosphatase Inhibitor Cocktails (Thermo Fisher) and 50 U/ml RNAsin Plus (Promega). PNS was precleared with Sepharose beads for 60 min at 4°C and the pre-cleared lysate was incubated with washed antibody-bead complexes (DDX5 or control) for 3 h on a rotating wheel at 4°C. Supernatant was collected, depicting the unbound (UB) fraction. Beads were washed three times with RIP lysis buffer and one time with PBS. Proteins and RNA were eluted from the beads by incubation with RIP elution buffer [0.2% (w/v) SDS, 2% (v/v) β-mercaptoethanol in H_2O] for 5 min at 70°C and 800 rpm on a shaking device; 20% of supernatant in 1× SDS sample buffer was used for western blotting and 70% in Qiazol Lysis Reagent (Qiagen) for RNA analysis.

Fyn-dependent phosphorylation assays

Two days after transfection of Oli-*neu* cells with constitutive active (+) or kinase inactive (−) Fyn constructs (White et al., 2012), tyrosine-phosphorylated proteins were immunoprecipitated using 50 µl 4G10 antibody-coupled agarose bead slurry (Merck Millipore) according to the manufacturer's instructions. Precleared Oli-*neu* lysates were prepared as described above and incubated with 4G10 beads for 4 h on a rotating wheel at 4°C. Beads were washed four times with lysis buffer, once with PBS and proteins were eluted by the addition of 2× sample buffer with 400 mM DTT for 5 min at 90°C. Proteins were resolved by SDS-PAGE and analyzed by western blotting.

For recombinant Fyn kinase assays, endogenous DDX5 and hnRNP A2/B1 were immunopurified as described above, carrying out 4 washing steps. Washing step 3 was performed using kinase buffer [50 mM 1,4-Piperazinediethanesulfonic acid (PIPES), pH 7.02, 10 mM $MgCl_2$] and step 4 with kinase buffer containing 50 µM ATP. Per assay, 30 ng active recombinant human Fyn (Fyn A, active; SignalChem) were added to the beads in 40 µl kinase buffer with 50 µM ATP. As control condition, the kinase was replaced with an equal amount of dH_2O. The assay was carried out incubating the beads for 20 min at 30°C and 800 rpm on a shaking device. The reaction was stopped and the proteins were eluted by the addition of 15 µl of 4× sample buffer and heating for 5 min at 90°C at 800 rpm on a shaking device. Phosphorylated proteins were analyzed by SDS-PAGE and western blotting.

Single-molecule fluorescent *in situ* hybridization (smFISH) and immunocytochemistry

MACS-isolated primary oligodendrocytes were fixed with Roti Histofix 4% (w/v) formaldehyde (Roth) for 15 min at RT and smFISH was performed using Panomics QuantiGene ViewRNA ISH Cell Assay (Affimetrix) with probe sets targeting murine *Mbp* transcripts (#VB1-13861-TYPE1) according to the manufacturer's protocol, omitting Proteinase K treatment. Following smFISH, immunofluorescence staining of indicated protein antigens was accomplished as described before (White et al., 2012). Briefly, nonspecific binding was blocked with PBS containing 10% (v/v) HS, primary antibodies were incubated in blocking solution overnight at 4°C and detection was carried out with species-matching pre-adsorbed Fluorophore-conjugated secondary antibodies (Invitrogen/Dianova). Alternatively, smFISH was performed using the Stellaris smFISH system (Biosearchtech). A Stellaris custom FISH probe library (46 fluorescent antisense probes) was designed covering the sequence of murine *Mbp* CDS, excluding the exons 2, 5 and 6 and *in situ* hybridization was performed according to the manufacturer's suggestions. Coverslips were mounted in Mowiol or ProLong Diamond Antifade Mountant (Life Technologies).

Microscopy and image analysis

Fluorescently labeled cells were imaged with a DFC360 FX camera, using a Leica DM6000B wide-field microscope. Confocal images were taken using a Leica TCS SP5 laser scanning microscope. Images were processed with ImageJ v.1.51d and Adobe Photoshop.

RNA granule separation using Optiprep density gradient centrifugation

Density gradient centrifugation was performed according to the protocol established by Daniela Karra to isolate RNP complexes from brain lysates (Fritzsche et al., 2013). MACS-sorted (anti-O4) primary oligodendrocytes at DIV 5 were lysed in RIP lysis buffer, PNS was loaded on 5-25% Optiprep (Sigma) density gradients and centrifuged for 2.5 h at 280,000 ***g*** at 4°C in an ultracentrifuge, using a SW41-Ti Rotor (Beckmann Coulter). Gradients were prepared under RNase-free conditions in lysis buffer and were allowed to establish by horizontal diffusion for 1 h at 4°C. Optionally, RNase treatment of the lysates with 50 µg/ml RNase A (Invitrogen) for 20 min at 30°C was performed to disrupt RNP complexes. Fractions were collected from the top of the gradient and proteins were analyzed by western blotting. Additionally, total RNA was extracted from each fraction and the abundance of specific mRNAs relative to the Input was determined by qRT-PCR as described above.

Nanofiber differentiation assay

Primary OPCs were isolated by MACS sorting using NG2-coupled magnetic beads (MIltenyi) and seeded in 12-well plates containing half a nanofiber multiwell plate insert (#Z694614 Sigma, Nanofiber solutions) with aligned 700-nm-diameter electrospun polycaprolactone (PCL) fibers. Wells and nanofiber inserts were coated with poly-L-lysine and MACS-sorted cells ($NG2^+$) were plated in OPC medium on the day before transfection of indicated siRNA cocktails using the Lipofectamine RNAiMAX Transfection Reagent (Thermo Fisher Scientific). Medium was exchanged with differentiation medium (MACS Neuro medium, Miltenyi) supplemented with 1× NeuroBrew21 (Miltenyi), penicillin-streptomycin (100 U/ml, Life Technologies), L-glutamine (2 mM, Life Technologies), Forskolin (4.2 µg/ml, Sigma), CNTF (10 ng/ml, Pepro Tech), T3 (40 ng/ml, Sigma) after 6 h and subsequently every second day. After 5 days of differentiation on nanofiber inserts, cells were fixed in 4% (w/v) paraformaldehyde for 20 min at RT followed by immunocytochemistry. Remaining cells in the other half of the 12-well plate were lysed and used for western blotting.

Immunocytochemistry was performed as described above for cells on coverslips with minor modifications. Washing steps were extended to 5 min each with 0.01% (v/v) Triton X-100 in PBS once and PBS twice following the antibody incubations. To circumvent detection of false-positive cells from background signals, only cell nuclei double-positive for Olig2 and DAPI were considered as $Olig2^+$ oligodendrocytes and are displayed and counted as binary images using Image J. In addition, $Olig2^+$ oligodendrocytes were manually counted for the expression of MBP and $MBP^+/Olig2^+$ double positive cells were normalized to total $Olig2^+$ cell numbers. To obtain the longitudinal MBP^+ process extension on the nanofibers, the maximal distance of the cellular MBP signal from the cell nucleus border was measured in parallel to the common nanofiber orientation. Regions were only taken into account where they were clearly distinguishable as belonging to individual cells, and measurement of angle and MBP extension distance was performed using ImageJ.

Statistics

Independent experiments using primary cells are defined as separately isolated cell populations from individual animal groups. Independent experiments using Oli-*neu* are defined as separately cultured cells for each experiment. Statistical analysis of the experimental datasets was applied using Microsoft Excel or GraphPad Prism 7 (GraphPad software). Statistical tests were selected according to the type of data and are indicated in the corresponding figure legends together with calculated *P*-values.

Acknowledgements

We thank Dr Daniela Karra for help with initial Optiprep density centrifugation, Dr William Rigby for providing hnRNP A2/B1 antibodies (clone EF67), Dr Sandra Ritz and the IMB Mainz Core Facility Microscopy, Prof. Tanja Kuhlmann for critical discussion and assistance with the nanofiber cultures and Ulrike Stapf, Lilja Niedens and Cornelia Braun for competent technical assistance.

Competing interests

The authors declare no competing or financial interests.

Author contributions

Conceptualization: P.H.-K., R.W., E.-M.K.-A., J.T., C.G.; Formal analysis: P.H.-K., C.G.; Investigation: P.H., R.W., S.T., C.G.; Resources: S.T., E.-M.K.-A., J.T.; Writing - original draft: P.H.-K., J.T., C.G.; Writing - review & editing: P.H.-K., R.W., S.T., E.-M.K.-A., J.T., C.G.; Visualization: P.H.-K., R.W., C.G.; Supervision: E.-M.K.-A., J.T., C.G.; Project administration: J.T., C.G.; Funding acquisition: J.T.

Funding

This work was supported by the Deutsche Forschungsgemeinschaft (SFB CRC TR 128 Project B7 to J.T., Grant GRK 1044 to J.T., SPP 1738 WH 168/3-1 to R.W.) and by the Forschungszentrum für Immunotherapie (FZI) of the Johannes Gutenberg-University Mainz (to S.T.).

Supplementary information

Supplementary information available online at
http://jcs.biologists.org/lookup/doi/10.1242/jcs.204750.supplemental

References

Aggarwal, S., Yurlova, L., Snaidero, N., Reetz, C., Frey, S., Zimmermann, J., Pahler, G., Janshoff, A., Friedrichs, J., Müller, D. J. et al. (2011). A size barrier limits protein diffusion at the cell surface to generate lipid-rich myelin-membrane sheets. *Dev. Cell* **21**, 445-456.

Aggarwal, S., Snaidero, N., Pähler, G., Frey, S., Sanchez, P., Zweckstetter, M., Janshoff, A., Schneider, A., Weil, M. T., Schaap, I. A. et al. (2013). Myelin membrane assembly is driven by a phase transition of myelin basic proteins into a cohesive protein meshwork. *PLoS Biol.* **11**, e1001577.

Ainger, K., Avossa, D., Morgan, F., Hill, S. J., Barry, C., Barbarese, E. and Carson, J. H. (1993). Transport and localization of exogenous myelin basic protein mRNA microinjected into oligodendrocytes. *J. Cell Biol.* **123**, 431-441.

Ainger, K., Avossa, D., Diana, A. S., Barry, C., Barbarese, E. and Carson, J. H. (1997). Transport and localization elements in myelin basic protein mRNA. *J. Cell Biol.* **138**, 1077-1087.
Allinquant, B., Staugaitis, S. M., D'urso, D. and Colman, D. R. (1991). The ectopic expression of myelin basic protein isoforms in Shiverer oligodendrocytes: implications for myelinogenesis. *J. Cell Biol.* **113**, 393-403.
Anderson, P. and Kedersha, N. (2009). RNA granules: post-transcriptional and epigenetic modulators of gene expression. *Nat. Rev. Mol. Cell Biol.* **10**, 430-436.
Bakhti, M., Aggarwal, S. and Simons, M. (2014). Myelin architecture: zippering membranes tightly together. *Cell. Mol. Life Sci.* **71**, 1265-1277.
Barbarese, E., Carson, J. H. and Braun, P. E. (1978). Accumulation of the four myelin basic proteins in mouse brain during development. *J. Neurochem.* **31**, 779-782.
Barbarese, E., Koppel, D. E., Deutscher, M. P., Smith, C. L., Ainger, K., Morgan, F. and Carson, J. H. (1995). Protein translation components are colocalized in granules in oligodendrocytes. *J. Cell Sci.* **108**, 2781-2790.
Barbarese, E., Brumwell, C., Kwon, S., Cui, H. and Carson, J. H. (1999). RNA on the road to myelin. *J. Neurocytol.* **28**, 263-270.
Bauer, N. M., Moos, C., Van Horssen, J., Witte, M., Van Der Valk, P., Altenhein, B., Luhmann, H. J. and White, R. (2012). Myelin basic protein synthesis is regulated by small non-coding RNA 715. *EMBO Rep.* **13**, 827-834.
Bechler, M. E., Byrne, L. and Ffrench-Constant, C. (2015). CNS myelin sheath lengths are an intrinsic property of oligodendrocytes. *Curr. Biol.* **25**, 2411-2416.
Bercury, K. K. and Macklin, W. B. (2015). Dynamics and mechanisms of CNS myelination. *Dev. Cell* **32**, 447-458.
Boccaccio, G. L. (2000). Targeting of mRNAs within the glial cell cytoplasm: how to hide the message along the journey. *J. Neurosci. Res.* **62**, 473-479.
Boggs, J. M. (2006). Myelin basic protein: a multifunctional protein. *Cell. Mol. Life Sci.* **63**, 1945-1961.
Buchan, J. R. (2014). mRNP granules. Assembly, function, and connections with disease. *RNA Biol.* **11**, 1019-1030.
Camats, M., Guil, S., Kokolo, M. and Bach-Elias, M. (2008). P68 RNA helicase (DDX5) alters activity of cis- and trans-acting factors of the alternative splicing of H-Ras. *PLoS ONE* **3**, e2926.
Campagnoni, A. T., Pribyl, T. M., Campagnoni, C. W., Kampf, K., Amur-Umarjee, S., Landry, C. F., Handley, V. W., Newman, S. L., Garbay, B. and Kitamura, K. (1993). Structure and developmental regulation of Golli-mbp, a 105-kilobase gene that encompasses the myelin basic protein gene and is expressed in cells in the oligodendrocyte lineage in the brain. *J. Biol. Chem.* **268**, 4930-4938.
Capello, E., Voskuhl, R. R., Mcfarland, H. F. and Raine, C. S. (1997). Multiple sclerosis: re-expression of a developmental gene in chronic lesions correlates with remyelination. *Ann. Neurol.* **41**, 797-805.
Carson, J. H., Worboys, K., Ainger, K. and Barbarese, E. (1997). Translocation of myelin basic protein mRNA in oligodendrocytes requires microtubules and kinesin. *Cell Motil. Cytoskelet.* **38**, 318-328.
Carson, J. H., Gao, Y., Tatavarty, V., Levin, M. K., Korza, G., Francone, V. P., Kosturko, L. D., Maggipinto, M. J. and Barbarese, E. (2008). Multiplexed RNA trafficking in oligodendrocytes and neurons. *Biochim. Biophys. Acta* **1779**, 453-458.
Colman, D. R., Kreibich, G., Frey, A. B. and Sabatini, D. D. (1982). Synthesis and incorporation of myelin polypeptides into CNS myelin. *J. Cell Biol.* **95**, 598-608.
Compston, A. and Coles, A. (2008). Multiple sclerosis. *Lancet* **372**, 1502-1517.
Dardenne, E., Polay Espinoza, M., Fattet, L., Germann, S., Lambert, M. P., Neil, H., Zonta, E., Mortada, H., Gratadou, L., Deygas, M. et al. (2014). RNA helicases DDX5 and DDX17 dynamically orchestrate transcription, miRNA, and splicing programs in cell differentiation. *Cell Rep.* **7**, 1900-1913.
De Vries, H., De Jonge, J. C., Schrage, C., Van Der Haar, M. E. and Hoekstra, D. (1997). Differential and cell development-dependent localization of myelin mRNAs in oligodendrocytes. *J. Neurosci. Res.* **47**, 479-488.
Duncan, I. D. and Radcliff, A. B. (2016). Inherited and acquired disorders of myelin: the underlying myelin pathology. *Exp. Neurol.* **283**, 452-475.
Dyer, C. A., Philibotte, T. M., Billings-Gagliardi, S. and Wolf, M. K. (1995). Cytoskeleton in myelin-basic-protein-deficient shiverer oligodendrocytes. *Dev. Neurosci.* **17**, 53-62.
Eliscovich, C. and Singer, R. H. (2017). RNP transport in cell biology: the long and winding road. *Curr. Opin. Cell Biol.* **45**, 38-46.
Elvira, G., Wasiak, S., Blandford, V., Tong, X.-K., Serrano, A., Fan, X., del Rayo Sánchez-Carbente, M., Servant, F., Bell, A. W., Boismenu, D. et al. (2006). Characterization of an RNA granule from developing brain. *Mol. Cell. Proteomics* **5**, 635-651.
Ettle, B., Schlachetzki, J. C. and Winkler, J. (2015). Oligodendroglia and myelin in neurodegenerative diseases: more than just bystanders? *Mol. Neurobiol.* **53**, 3046-3062.
Ffrench-Constant, C. (1994). Pathogenesis of multiple sclerosis. *Lancet* **343**, 271-275.
Fields, R. D. (2008). White matter in learning, cognition and psychiatric disorders. *Trends Neurosci.* **31**, 361-370.
Fields, R. D. (2015). A new mechanism of nervous system plasticity: activity-dependent myelination. *Nat. Rev. Neurosci.* **16**, 756-767.
Fitzner, D., Schneider, A., Kippert, A., Möbius, W., Willig, K. I., Hell, S. W., Bunt, G., Gaus, K. and Simons, M. (2006). Myelin basic protein-dependent plasma membrane reorganization in the formation of myelin. *EMBO J.* **25**, 5037-5048.
Francone, V. P., Maggipinto, M. J., Kosturko, L. D. and Barbarese, E. (2007). The microtubule-associated protein tumor overexpressed gene/cytoskeleton-associated protein 5 is necessary for myelin basic protein expression in oligodendrocytes. *J. Neurosci.* **27**, 7654-7662.
Franklin, R. J. and Goldman, S. A. (2015). Glia disease and repair-remyelination. *Cold Spring Harbor Perspect. Biol.* **7**, a020594.
Franklin, R. J., Ffrench-Constant, C., Edgar, J. M. and Smith, K. J. (2012). Neuroprotection and repair in multiple sclerosis. *Nat. Rev. Neurol.* **8**, 624-634.
Fritzsche, R., Karra, D., Bennett, K. L., Ang, F. Y., Heraud-Farlow, J. E., Tolino, M., Doyle, M., Bauer, K. E., Thomas, S., Planyavsky, M. et al. (2013). Interactome of two diverse RNA granules links mRNA localization to translational repression in neurons. *Cell Rep.* **5**, 1749-1762.
Fuller-Pace, F. V. (2013). The DEAD box proteins DDX5 (p68) and DDX17 (p72): multi-tasking transcriptional regulators. *Biochim. Biophys. Acta* **1829**, 756-763.
Gao, Y., Tatavarty, V., Korza, G., Levin, M. K. and Carson, J. H. (2008). Multiplexed dendritic targeting of alpha calcium calmodulin-dependent protein kinase II, neurogranin, and activity-regulated cytoskeleton-associated protein RNAs by the A2 pathway. *Mol. Biol. Cell* **19**, 2311-2327.
Geißler, V., Altmeyer, S., Stein, B., Uhlmann-Schiffler, H. and Stahl, H. (2013). The RNA helicase Ddx5/p68 binds to hUpf3 and enhances NMD of Ddx17/p72 and Smg5 mRNA. *Nucleic Acids Res.* **41**, 7875-7888.
Gonsior, C., Biname, F., Fruhbeis, C., Bauer, N. M., Hoch-Kraft, P., Luhmann, H. J., Trotter, J. and White, R. (2014). Oligodendroglial p130Cas is a target of Fyn kinase involved in process formation, cell migration and survival. *PLoS ONE* **9**, e89423.
Haimovich, G., Choder, M., Singer, R. H. and Trcek, T. (2013). The fate of the messenger is pre-determined: a new model for regulation of gene expression. *Biochim. Biophys. Acta* **1829**, 643-653.
Han, S. P., Friend, L. R., Carson, J. H., Korza, G., Barbarese, E., Maggipinto, M., Hatfield, J. T., Rothnagel, J. A. and Smith, R. (2010). Differential subcellular distributions and trafficking functions of hnRNP A2/B1 spliceoforms. *Traffic* **11**, 886-898.
Harauz, G. and Boggs, J. M. (2013). Myelin management by the 18.5-kDa and 21.5-kDa classic myelin basic protein isoforms. *J. Neurochem.* **125**, 334-361.
Hardy, R. J., Lazzarini, R. A., Colman, D. R. and Friedrich, V. L. Jr (1996). Cytoplasmic and nuclear localization of myelin basic proteins reveals heterogeneity among oligodendrocytes. *J. Neurosci. Res.* **46**, 246-257.
Herbert, A. L., Fu, M.-m., Drerup, C. M., Gray, R. S., Harty, B. L., Ackermann, S. D., O'reilly-Pol, T., Johnson, S. L., Nechiporuk, A. V., Barres, B. A., et al. (2017). Dynein/dynactin is necessary for anterograde transport of Mbp mRNA in oligodendrocytes and for myelination in vivo. *Proc. Natl. Acad. Sci. USA* **114**, E9153-E9162.
Hoek, K. S., Kidd, G. J., Carson, J. H. and Smith, R. (1998). hnRNP A2 selectively binds the cytoplasmic transport sequence of myelin basic protein mRNA. *Biochemistry* **37**, 7021-7029.
Hong, S., Noh, H., Chen, H., Padia, R., Pan, Z. K., Su, S. B., Jing, Q., Ding, H. F. and Huang, S. (2013). Signaling by p38 MAPK stimulates nuclear localization of the microprocessor component p68 for processing of selected primary microRNAs. *Sci. Signal.* **6**, ra16.
Hughes, E. G. and Appel, B. (2016). The cell biology of CNS myelination. *Curr. Opin. Neurobiol.* **39**, 93-100.
Jalal, C., Uhlmann-Schiffler, H. and Stahl, H. (2007). Redundant role of DEAD box proteins p68 (Ddx5) and p72/p82 (Ddx17) in ribosome biogenesis and cell proliferation. *Nucleic Acids Res.* **35**, 3590-3601.
Jung, M., Krämer, E., Grzenkowski, M., Tang, K., Blakemore, W., Aguzzi, A., Khazaie, K., Chlichlia, K., Von Blankenfeld, G., Kettenmann, H. et al. (1995). Lines of murine oligodendroglial precursor cells immortalized by an activated neu tyrosine kinase show distinct degrees of interaction with axons in vitro and in vivo. *Eur. J. Neurosci.* **7**, 1245-1265.
Kanai, Y., Dohmae, N. and Hirokawa, N. (2004). Kinesin transports RNA: isolation and characterization of an RNA-transporting granule. *Neuron* **43**, 513-525.
Kang, S. H., Li, Y., Fukaya, M., Lorenzini, I., Cleveland, D. W., Ostrow, L. W., Rothstein, J. D. and Bergles, D. E. (2013). Degeneration and impaired regeneration of gray matter oligodendrocytes in amyotrophic lateral sclerosis. *Nat. Neurosci.* **16**, 571-579.
Kar, A., Fushimi, K., Zhou, X., Ray, P., Shi, C., Chen, X., Liu, Z., Chen, S. and Wu, J. Y. (2011). RNA helicase p68 (DDX5) regulates tau exon 10 splicing by modulating a stem-loop structure at the 5′ splice site. *Mol. Cell. Biol.* **31**, 1812-1821.
Kost, G. C., Yang, M. Y., Li, L., Zhang, Y., Liu, C. Y., Kim, D. J., Ahn, C. H., Lee, Y. B. and Liu, Z. R. (2015). A novel anti-cancer agent, 1-(3,5-Dimethoxyphenyl)-4-[(6-Fluoro-2-Methoxyquinoxalin-3-yl)Aminocarbonyl] Piperazine (RX-5902), interferes with beta-catenin function through Y593 Phospho-p68 RNA Helicase. *J. Cell. Biochem.* **116**, 1595-1601.
Kosturko, L. D., Maggipinto, M. J., D'sa, C., Carson, J. H. and Barbarese, E. (2005). The microtubule-associated protein tumor overexpressed gene binds to

the RNA trafficking protein heterogeneous nuclear ribonucleoprotein A2. *Mol. Biol. Cell* **16**, 1938-1947.
Kosturko, L. D., Maggipinto, M. J., Korza, G., Lee, J. W., Carson, J. H. and Barbarese, E. (2006). Heterogeneous nuclear ribonucleoprotein (hnRNP) E1 binds to hnRNP A2 and inhibits translation of A2 response element mRNAs. *Mol. Biol. Cell* **17**, 3521-3533.
Kuhlmann, T., Miron, V., Cuo, Q., Wegner, C., Antel, J. and Bruck, W. (2008). Differentiation block of oligodendroglial progenitor cells as a cause for remyelination failure in chronic multiple sclerosis. *Brain* **131**, 1749-1758.
Larocque, D., Pilotte, J., Chen, T., Cloutier, F., Massie, B., Pedraza, L., Couture, R., Lasko, P., Almazan, G. and Richard, S. (2002). Nuclear retention of MBP mRNAs in the quaking viable mice. *Neuron* **36**, 815-829.
Laursen, L. S., Chan, C. W. and Ffrench-Constant, C. (2009). An integrin-contactin complex regulates CNS myelination by differential Fyn phosphorylation. *J. Neurosci.* **29**, 9174-9185.
Laursen, L. S., Chan, C. W. and Ffrench-Constant, C. (2011). Translation of myelin basic protein mRNA in oligodendrocytes is regulated by integrin activation and hnRNP-K. *J. Cell Biol.* **192**, 797-811.
Lee, S., Leach, M. K., Redmond, S. A., Chong, S. Y., Mellon, S. H., Tuck, S. J., Feng, Z. Q., Corey, J. M. and Chan, J. R. (2012). A culture system to study oligodendrocyte myelination processes using engineered nanofibers. *Nat. Methods* **9**, 917-922.
Lin, C., Yang, L., Yang, J. J., Huang, Y. and Liu, Z.-R. (2005). ATPase/helicase activities of p68 RNA helicase are required for pre-mRNA splicing but not for assembly of the spliceosome. *Mol. Cell. Biol.* **25**, 7484-7493.
Linder, P. and Jankowsky, E. (2011). From unwinding to clamping - the DEAD box RNA helicase family. *Nat. Rev. Mol. Cell Biol.* **12**, 505-516.
Lu, Z., Ku, L., Chen, Y. and Feng, Y. (2005). Developmental abnormalities of myelin basic protein expression in fyn knock-out brain reveal a role of Fyn in posttranscriptional regulation. *J. Biol. Chem.* **280**, 389-395.
Lyons, D. A., Naylor, S. G., Scholze, A. and Talbot, W. S. (2009). Kif1B is essential for mRNA localization in oligodendrocytes and development of myelinated axons. *Nat. Genet.* **41**, 854-858.
Ma, W. K., Cloutier, S. C. and Tran, E. J. (2013). The DEAD-box protein Dbp2 functions with the RNA-binding protein Yra1 to promote mRNP assembly. *J. Mol. Biol.* **425**, 3824-3838.
Maggipinto, M. J., Ford, J., Le, K. H., Tutolo, J. W., Furusho, M., Wizeman, J. W., Bansal, R. and Barbarese, E. (2017). Conditional knockout of TOG results in CNS hypomyelination. *Glia* **7**, 23106.
Martinez, F. J., Pratt, G. A., Van Nostrand, E. L., Batra, R., Huelga, S. C., Kapeli, K., Freese, P., Chun, S. J., Ling, K., Gelboin-Burkhart, C. et al. (2016). Protein-RNA networks regulated by normal and ALS-associated mutant HNRNPA2B1 in the nervous system. *Neuron* **13**, 30655-30659.
Merz, C., Urlaub, H., Will, C. L. and Luhrmann, R. (2007). Protein composition of human mRNPs spliced in vitro and differential requirements for mRNP protein recruitment. *RNA* **13**, 116-128.
Miron, V. E., Kuhlmann, T. and Antel, J. P. (2011). Cells of the oligodendroglial lineage, myelination, and remyelination. *Biochim. Biophys. Acta* **1812**, 184-193.
Mitew, S., Hay, C. M., Peckham, H., Xiao, J., Koenning, M. and Emery, B. (2014). Mechanisms regulating the development of oligodendrocytes and central nervous system myelin. *Neuroscience* **276**, 29-47.
Moore, M. J. and Proudfoot, N. J. (2009). Pre-mRNA processing reaches back to transcription and ahead to translation. *Cell* **136**, 688-700.
Müller, C., Bauer, N. M., Schafer, I. and White, R. (2013). Making myelin basic protein -from mRNA transport to localized translation. *Front. Cell. Neurosci.* **7**, 169.
Müller, C., Schafer, I., Luhmann, H. J. and White, R. (2015). Oligodendroglial Argonaute protein Ago2 associates with molecules of the Mbp mRNA localization machinery and is a downstream target of Fyn kinase. *Front. Cell. Neurosci.* **9**, 328.
Munro, T. P., Magee, R. J., Kidd, G. J., Carson, J. H., Barbarese, E., Smith, L. M. and Smith, R. (1999). Mutational analysis of a heterogeneous nuclear ribonucleoprotein A2 response element for RNA trafficking. *J. Biol. Chem.* **274**, 34389-34395.
Nagasato, K., Farris, R. W., II, Dubois-Dalcq, M. and Voskuhl, R. R. (1997). Exon 2 containing myelin basic protein (MBP) transcripts are expressed in lesions of experimental allergic encephalomyelitis (EAE). *J. Neuroimmunol.* **72**, 21-25.
Nave, K. A. (2010). Myelination and support of axonal integrity by glia. *Nature* **468**, 244-252.
Nave, K. A. and Werner, H. B. (2014). Myelination of the nervous system: mechanisms and functions. *Annu. Rev. Cell Dev. Biol.* **30**, 503-533.
Nawaz, S., Sanchez, P., Schmitt, S., Snaidero, N., Mitkovski, M., Velte, C., Bruckner, B. R., Alexopoulos, I., Czopka, T., Jung, S. Y. et al. (2015). Actin filament turnover drives leading edge growth during myelin sheath formation in the central nervous system. *Dev. Cell* **34**, 139-151.
Ozgen, H., Kahya, N., De Jonge, J. C., Smith, G. S., Harauz, G., Hoekstra, D. and Baron, W. (2014). Regulation of cell proliferation by nucleocytoplasmic dynamics of postnatal and embryonic exon-II-containing MBP isoforms. *Biochim. Biophys. Acta* **1843**, 517-530.
Pedraza, L., Fidler, L., Staugaitis, S. M. and Colman, D. R. (1997). The active transport of myelin basic protein into the nucleus suggests a regulatory role in myelination. *Neuron* **18**, 579-589.
Poggi, G., Boretius, S., Mobius, W., Moschny, N., Baudewig, J., Ruhwedel, T., Hassouna, I., Wieser, G. L., Werner, H. B., Goebbels, S. et al. (2016). Cortical network dysfunction caused by a subtle defect of myelination. *Glia* **29**, 23039.
Purger, D., Gibson, E. M. and Monje, M. (2016). Myelin plasticity in the central nervous system. *Neuropharmacology* **110**, 563-573.
Raju, C. S., Goritz, C., Nord, Y., Hermanson, O., Lopez-Iglesias, C., Visa, N., Castelo-Branco, G. and Percipalle, P. (2008). In cultured oligodendrocytes the A/B-type hnRNP CBF-A accompanies MBP mRNA bound to mRNA trafficking sequences. *Mol. Biol. Cell* **19**, 3008-3019.
Readhead, C. and Hood, L. (1990). The dysmyelinating mouse mutations shiverer (shi) and myelin deficient (shimld). *Behav. Genet.* **20**, 213-234.
Salzman, D. W., Shubert-Coleman, J. and Furneaux, H. (2007). P68 RNA helicase unwinds the human let-7 microRNA precursor duplex and is required for let-7-directed silencing of gene expression. *J. Biol. Chem.* **282**, 32773-32779.
Samaan, S., Tranchevent, L. C., Dardenne, E., Polay Espinoza, M., Zonta, E., Germann, S., Gratadou, L., Dutertre, M. and Auboeuf, D. (2014). The Ddx5 and Ddx17 RNA helicases are cornerstones in the complex regulatory array of steroid hormone-signaling pathways. *Nucleic Acids Res.* **42**, 2197-2207.
Schafer, I., Muller, C., Luhmann, H. J. and White, R. (2016). MOBP levels are regulated by Fyn kinase and affect the morphological differentiation of oligodendrocytes. *J. Cell Sci.* **129**, 930-942.
Seiberlich, V., Bauer, N. G., Schwarz, L., Ffrench-Constant, C., Goldbaum, O. and Richter-Landsberg, C. (2015). Downregulation of the microtubule associated protein Tau impairs process outgrowth and myelin basic protein mRNA transport in oligodendrocytes. *Glia* **63**, 1621-1635.
Seiwa, C., Kojima-Aikawa, K., Matsumoto, I. and Asou, H. (2002). CNS myelinogenesis in vitro: myelin basic protein deficient shiverer oligodendrocytes. *J. Neurosci. Res.* **69**, 305-317.
Smith, G. S., Seymour, L. V., Boggs, J. M. and Harauz, G. (2012). The 21.5-kDa isoform of myelin basic protein has a non-traditional PY-nuclear-localization signal. *Biochem. Biophys. Res. Commun.* **422**, 670-675.
Smith, G. S., Samborska, B., Hawley, S. P., Klaiman, J. M., Gillis, T. E., Jones, N., Boggs, J. M. and Harauz, G. (2013). Nucleus-localized 21.5-kDa myelin basic protein promotes oligodendrocyte proliferation and enhances neurite outgrowth in coculture, unlike the plasma membrane-associated 18.5-kDa isoform. *J. Neurosci. Res.* **91**, 349-362.
Snaidero, N., Velte, C., Myllykoski, M., Raasakka, A., Ignatev, A., Werner, H. B., Erwig, M. S., Möbius, W., Kursula, P., Nave, K. A., et al. (2017). Antagonistic functions of MBP and CNP establish cytosolic channels in CNS myelin. *Cell Rep.* **18**, 314-323.
Staugaitis, S. M., Colman, D. R. and Pedraza, L. (1996). Membrane adhesion and other functions for the myelin basic proteins. *BioEssays* **18**, 13-18.
Suzuki, H. I., Yamagata, K., Sugimoto, K., Iwamoto, T., Kato, S. and Miyazono, K. (2009). Modulation of microRNA processing by p53. *Nature* **460**, 529-533.
Tanaka, T., Ishii, T., Mizuno, D., Mori, T., Yamaji, R., Nakamura, Y., Kumazawa, S., Nakayama, T. and Akagawa, M. (2011). (−)-Epigallocatechin-3-gallate suppresses growth of AZ521 human gastric cancer cells by targeting the DEAD-box RNA helicase p68. *Free Radic. Biol. Med.* **50**, 1324-1335.
Taniguchi, T., Iizumi, Y., Watanabe, M., Masuda, M., Morita, M., Aono, Y., Toriyama, S., Oishi, M., Goi, W. and Sakai, T. (2016). Resveratrol directly targets DDX5 resulting in suppression of the mTORC1 pathway in prostate cancer. *Cell Death Dis.* **7**, e2211.
Thakurela, S., Garding, A., Jung, R. B., Müller, C., Goebbels, S., White, R., Werner, H. B. and Tiwari, V. K. (2016). The transcriptome of mouse central nervous system myelin. *Sci. Rep.* **6**, 25828.
Torvund-Jensen, J., Steengaard, J., Reimer, L., Fihl, L. B. and Laursen, L. S. (2014). Transport and translation of MBP mRNA is regulated differently by distinct hnRNP proteins. *J. Cell Sci.* **127**, 1550-1564.
Ueki, T., Tsuruo, Y., Yamamoto, Y., Yoshimura, K., Takanaga, H., Seiwa, C., Motojima, K., Asou, H. and Yamamoto, M. (2012). A new monoclonal antibody, 4F2, specific for the oligodendroglial cell lineage, recognizes ATP-dependent RNA helicase Ddx54: possible association with myelin basic protein. *J. Neurosci. Res.* **90**, 48-59.
Wake, H., Lee, P. R. and Fields, R. D. (2011). Control of local protein synthesis and initial events in myelination by action potentials. *Science* **333**, 1647-1651.
Wake, H., Ortiz, F. C., Woo, D. H., Lee, P. R., Angulo, M. C. and Fields, R. D. (2015). Nonsynaptic junctions on myelinating glia promote preferential myelination of electrically active axons. *Nat. Commun.* **6**, 7844.
Wang, Y., Lacroix, G., Haines, J., Doukhanine, E., Almazan, G. and Richard, S. (2010). The QKI-6 RNA binding protein localizes with the MBP mRNAs in stress granules of glial cells. *PLoS ONE* **5**, e12824.
Wang, D., Huang, J. and Hu, Z. (2012). RNA helicase DDX5 regulates microRNA expression and contributes to cytoskeletal reorganization in basal breast cancer cells. *Mol. Cell. Proteomics* **11**, M111 011932.
White, R., Gonsior, C., Krämer-Albers, E. M., Stohr, N., Huttelmaier, S. and Trotter, J. (2008). Activation of oligodendroglial Fyn kinase enhances translation

of mRNAs transported in hnRNP A2-dependent RNA granules. *J. Cell Biol.* **181**, 579-586.

White, R., Gonsior, C., Bauer, N. M., Krämer-Albers, E. M., Luhmann, H. J. and Trotter, J. (2012). Heterogeneous nuclear ribonucleoprotein (hnRNP) F is a novel component of oligodendroglial RNA transport granules contributing to regulation of myelin basic protein (MBP) synthesis. *J. Biol. Chem.* **287**, 1742-1754.

Wigand, P., Tenzer, S., Schild, H. and Decker, H. (2009). Analysis of protein composition of red wine in comparison with rosé and white wines by electrophoresis and high-pressure liquid chromatography-mass spectrometry (HPLC-MS). *J. Agric. Food Chem.* **57**, 4328-4333.

Wu, J. I., Reed, R. B., Grabowski, P. J. and Artzt, K. (2002). Function of quaking in myelination: regulation of alternative splicing. *Proc. Natl. Acad. Sci. USA* **99**, 4233-4238.

Zhan, R., Yamamoto, M., Ueki, T., Yoshioka, N., Tanaka, K., Morisaki, H., Seiwa, C., Yamamoto, Y., Kawano, H., Tsuruo, Y. et al. (2013). A DEAD-box RNA helicase Ddx54 protein in oligodendrocytes is indispensable for myelination in the central nervous system. *J. Neurosci. Res.* **91**, 335-348.

Zuchero, J. B., Fu, M. M., Sloan, S. A., Ibrahim, A., Olson, A., Zaremba, A., Dugas, J. C., Wienbar, S., Caprariello, A. V., Kantor, C. et al. (2015). CNS myelin wrapping is driven by actin disassembly. *Dev. Cell* **34**, 152-167.